AD722667

R 721

Technical Report

# INTERFACE SLIP BEHAVIOR OF COMPOSITE PRESTRESSED CONCRETE BEAMS

April 1971

Sponsored by

NAVAL FACILITIES ENGINEERING COMMAND

NAVAL CIVIL ENGINEERING LABORATORY

Port Hueneme, California

Approved for public release; distribution unlimited.

Reproduced by
NATIONAL TECHNICAL
INFORMATION SERVICE
Springfield, Va. 22151

46

## INTRODUCTION

### General

Composite prestressed concrete construction is an attempt to improve the economy of, but maintain the advantages of, normal prestressed concrete. Composite concrete should combine the economy and efficiency of mass production of standardized units with the strength and ductility of monolithic structures. The potential benefits to be derived from this type of construction are threefold: (1) the strength of the cast-in-situ concrete need not be as high as that for the precast portion, (2) the prestressing force required to prestress the precast section will be less than that for the overall section, (3) the precast units can be used as permanent forms, thus eliminating costly shoring.

However, it is essential that the precast and cast-in-situ elements of a composite member act together as a unit for all expected loading conditions. Adequate bond at the interface between the precast and the cast-in-situ elements is required to insure that the composite section realizes the same capacity as a monolithic section with similar properties. The mode of failure should be a ductile one in the event of excessive loading. The ductile behavior will provide adequate warning of impending difficulties, which may furnish opportunities to take corrective measures and prevent a catastrophic collapse. When a concrete member is properly designed, reinforcing steel provides the desired ductility. The evaluation of the shear strength at the interface between precast and cast-in-situ concrete has been the subject of some research. However, the ultimate strength of shear transfer between composite-beam elements has not been well defined because of the limited number of failures due to interface shear. Reference 1 contains a list of references to investigations of more general composite beams and to discussions of the general hypothesis of failure.

This study is an extension of the work presented in Reference 1. A special composite beam known as a "split beam" was used as a test specimen. The split-beam concept was proposed by A. Amirikian.[2] The objective of this concept is to minimize the amount of prestressing force by prestressing only that part of the beam which will be subjected to tensile stress under live load. The interface between the precast and cast-in-situ elements is positioned at the centroid of the composite section, where it will be required to transfer the maximum horizontal shear stresses. The design concept of split beams is presented in References 1 and 2.

**INTERFACE SLIP BEHAVIOR OF COMPOSITE PRESTRESSED CONCRETE BEAMS**

Technical Report R-721

YF 38.534.001.01.009

by

S. B. Nosseir and G. E. Warren

## ABSTRACT

This report deals with the interface shear strength and slip behavior of posttensioned concrete composite beams. The interface between the two composite elements was positioned on the centroidal axis of the composite cross section. Eleven simply supported beams with 8-foot spans were statically loaded to failure. The effect of interface roughness and web reinforcement on relative slip between the composite elements was studied. Web reinforcement crossing the interface and roughness of interface decreased the rate of relative slip and allowed increased magnitudes of slip before failure. Interface roughness and web steel improved the integrity, strength, and energy-absorption capacity of the composite beams. The ultimate interface shear resistances determined from the tests were higher than those recommended by the ACI code.

ACCESSION for
GFSTI
A

Approved for public release; distribution unlimited.

Copies available at the National Technical Information Service (NTIS), Sills Building, 5285 Port Royal Road, Springfield, Va. 22151

### Objective

The objective of this study was to investigate the shear transfer across the interface between the precast-prestressed and the cast-in-situ elements of the prestressed split beam. Specifically, information was to be determined about the effect of interface roughness as well as amount, strength, and distribution of web reinforcement crossing the interface on the failure mode and interface slip characteristics. Slip characteristics included load-slip traits, slip distribution, and magnitude of slip at failure.

Although the study utilized the split beam as a test specimen, the results are applicable to the broad class of composite construction. Recommendations were to be made with regard to the safe design of shear transfer across the interface of the composite concrete-to-concrete beams.

### Scope

Eleven prestressed concrete split beams were statically loaded to failure. The beams had I-sections with the interface between the precast and cast-in-situ elements positioned near the composite-section centroid. Eight beams had smooth trowel-finished interface surfaces, while the remaining three had rough wire-brushed surfaces. The specimen was similar to the one used in Reference 1, but had a larger cross section with a 50% increase in depth.

The web reinforcement was varied by changing the stirrup size, spacing, and yield strength. Stirrups were fabricated from 8- and 12-gage wire. The percentage of web reinforcement crossing the interface, r, varied from 0 to 1.03%, while $rf_y$ varied from 0 to 317.5 psi.

For load—slip characteristics and slip distribution, relative slip between beam elements was measured by slip devices positioned at regular intervals along the portion of the beam span between the load point and reaction (shear span).

## EXPERIMENTAL PROGRAM AND PROCEDURE

### Test Specimen

The test specimens were posttensioned I-beams. Each was 9 feet in overall length, had an 8-foot simply supported span, and was loaded at two points producing a shear span of 27 inches. Figure 1 indicates the nominal beam cross section, location of the prestressing tendon, and the positions of supports and load points for tests.

## CONTENTS


page

INTRODUCTION . . . . . 1

General . . . . . 1

Objective . . . . . 2

Scope . . . . . 2

EXPERIMENTAL PROGRAM AND PROCEDURE . . . . . 2

Test Specimen . . . . . 2

Materials . . . . . 4

Fabrication . . . . . 8

Test Equipment and Procedure . . . . . 11

RESULTS AND DISCUSSION . . . . . 14

General . . . . . 14

Beam Behavior and Mode of Failure . . . . . 17

Deflection . . . . . 21

Ultimate Strength and Interface Shear Stress . . . . . 21

Slip . . . . . 27

SUMMARY AND CONCLUSIONS . . . . . 34

DESIGN RECOMMENDATIONS . . . . . 35

REFERENCES . . . . . 36

LIST OF SYMBOLS . . . . . 39

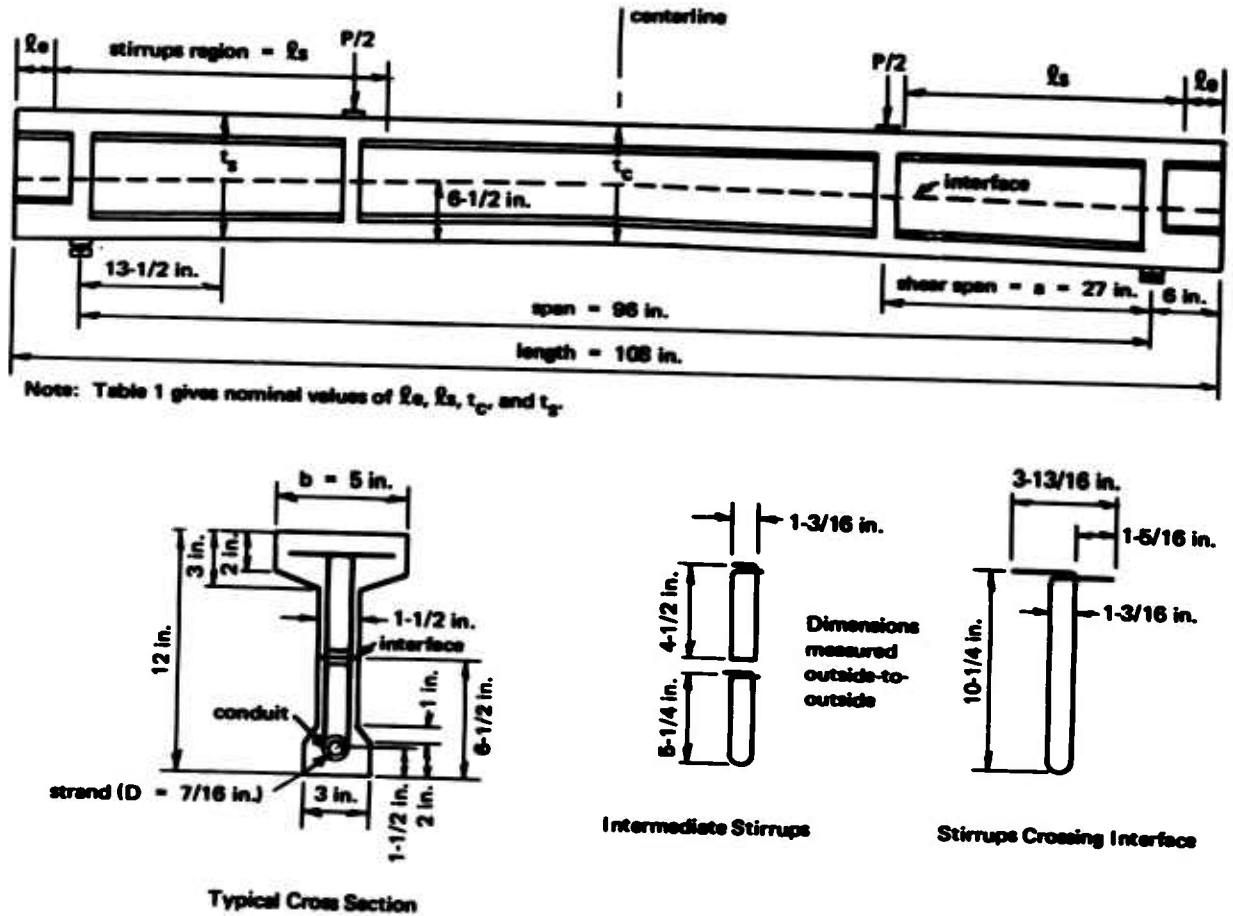


Figure 1. Details of test beams.

In order to utilize the split-beam concept, the centroidal axis for the overall section was determined. This axis became the interface between the composite elements of the beam. The shape of the cross section and the selection of the interface at the centroidal axis of the overall section enhanced the possibility of interface shear failure prior to flexural or diagonal modes of failure.

That portion of the composite beam that was precast and prestressed was designated the precast element. The portion of the beam which resisted the compressive stresses under loading was cast onto the precast element and was termed the cast-in-situ element.

The prestressing cables were placed in conduits which were thin-walled steel tubing with 7/8-inch outside diameter and 0.035-inch wall thickness. The tubing was tied into position at the ends and the load points. The conduit was straight and placed at a constant depth throughout the beam length (1-1/2 inches from the bottom of the beam to the center of the conduit).

Cages were fabricated by tying stirrups to the thin-wall steel conduit as shown in the photograph of Figure 2. Stirrups extended around the conduit and were anchored in the flange of the cast-in-situ element. These stirrups provided the primary parameter for resistance to interface shear failure. In addition to these stirrups, short intermediate ones were placed in both composite elements to strengthen the beam against a diagonal tension failure. In the specimens with no stirrups crossing the interface, only the short stirrups were used.

The test beams are designated by a letter-numeral identification according to the interface condition (for example, S1.04AI). The first letter indicates whether the interface was wire brushed, R, or trowelled smooth, S. The numeral following this letter denotes the percentage of web reinforcement crossing the interface. The letter following the numeral is the designation for the size of the stirrups crossing the interface—the letter A indicates 12-gage and B indicates 8-gage stirrups. If no stirrups crossed the interface, then 0.00 was specified and the letter referring to the size was omitted. The final letter indicates the type of failure; the letter D indicates diagonal tension, F indicates flexure, and I indicates interface shear.

## Materials

**Concrete.** The mix design for the concrete was based on the recommendations given in Reference 3. The concrete was a mixture of Type III portland cement, Santa Clara River sand, and Port Hueneme city water. A cumulative gradation curve for the sand is shown in Figure 3. Concrete mixes and strengths for all beams are listed in Table 2.

Table 1. Properties of Test Beams*

| Beam Designation | Condition of Interface | $t_s$ (in.) | $t_c$ (in.) | $d_s$ (in.) | $d_c$ (in.) | $\frac{a}{d_s}$ | p (%) | Stirrup Data | | | | | | | |
|---|---|---|---|---|---|---|---|---|---|---|---|---|---|---|---|
| | | | | | | | | $\ell_e$ (in.) | $\ell_s$ (in.) | D (in.) | s (in.) | $r_l$ (%) | r (%) | $f_y$ (ksi) | $rf_y$ (ps |
| S0.00I | smooth | 11.81 | 11.69 | 10.31 | 10.19 | 2.62 | 0.214 | – | – | – | – | 0.915 | 0 | – | – |
| R0.00I | rough | 11.81 | 11.69 | 10.31 | 10.19 | 2.62 | 0.214 | – | – | – | – | 0.915 | 0 | – | – |
| S0.26AI | smooth | 11.88 | 11.69 | 10.38 | 10.19 | 2.60 | 0.214 | 3.75 | 31.5 | 0.1055 | 4-1/2 | 0.259 | 0.259 | 21.0 | 54. |
| S0.39AD | smooth | 11.81 | 11.69 | 10.31 | 10.19 | 2.62 | 0.214 | 4.5 | 30.0 | 0.1055 | 3 | 0.389 | 0.389 | 21.0 | 81. |
| S0.39AI | smooth | 11.78 | 11.53 | 10.28 | 10.03 | 2.63 | 0.217 | 4.5 | 30.0 | 0.1055 | 3 | 0.389 | 0.389 | 23.0 | 89. |
| S0.41BI | smooth | 11.75 | 11.59 | 10.25 | 10.09 | 2.63 | 0.216 | 2.63 | 33.75 | 0.1620 | 6-3/4 | 0.407 | 0.407 | 37.0 | 150. |
| S0.61BI | smooth | 11.75 | 11.66 | 10.25 | 10.16 | 2.63 | 0.215 | 3.75 | 31.5 | 0.1620 | 4-1/2 | 1.222 | 0.611 | 33.3 | 203. |
| R0.61BF | rough | 11.81 | 11.56 | 10.31 | 10.06 | 2.62 | 0.217 | 3.75 | 31.5 | 0.1620 | 4-1/2 | 1.222 | 0.611 | 33.3 | 203. |
| S0.92BI | smooth | 11.75 | 11.50 | 10.25 | 10.00 | 2.63 | 0.218 | 4.5 | 30.0 | 0.1620 | 3 | 1.830 | 0.915 | 34.7 | 317. |
| R0.92BF | rough | 11.81 | 11.63 | 10.31 | 10.13 | 2.62 | 0.215 | 4.5 | 30.0 | 0.1620 | 3 | 1.830 | 0.915 | 34.7 | 317. |
| S1.04AI | smooth | 11.81 | 11.69 | 10.31 | 10.19 | 2.62 | 0.214 | 5.44 | 29.125 | 0.1055 | 1-1/8 | 1.037 | 1.037 | 24.3 | 251. |

* See foldout list of symbols after References.

A

Table 1. Properties of Test Beams*

| Beam Designation | Condition of Interface | $t_s$ (in.) | $t_c$ (in.) | $d_s$ (in.) | $d_c$ (in.) | $\frac{a}{d_s}$ | p (%) | Stirrup Data | | | | | | | |
|---|---|---|---|---|---|---|---|---|---|---|---|---|---|---|---|
| | | | | | | | | $\ell_e$ (in.) | $\ell_s$ (in.) | D (in.) | s (in.) | $r_l$ (%) | r (%) | $f_y$ (ksi) | rf, (ps |
| S0.00I | smooth | 11.81 | 11.69 | 10.31 | 10.19 | 2.62 | 0.214 | – | – | – | – | 0.915 | 0 | – | – |
| R0.00I | rough | 11.81 | 11.69 | 10.31 | 10.19 | 2.62 | 0.214 | – | – | – | – | 0.915 | 0 | – | – |
| S0.26AI | smooth | 11.88 | 11.69 | 10.38 | 10.19 | 2.60 | 0.214 | 3.75 | 31.5 | 0.1055 | 4-1/2 | 0.259 | 0.259 | 21.0 | 54 |
| S0.39AD | smooth | 11.81 | 11.69 | 10.31 | 10.19 | 2.62 | 0.214 | 4.5 | 30.0 | 0.1055 | 3 | 0.389 | 0.389 | 21.0 | 81 |
| S0.39AI | smooth | 11.78 | 11.53 | 10.28 | 10.03 | 2.63 | 0.217 | 4.5 | 30.0 | 0.1055 | 3 | 0.389 | 0.389 | 23.0 | 89 |
| S0.41BI | smooth | 11.75 | 11.59 | 10.25 | 10.09 | 2.63 | 0.216 | 2.63 | 33.75 | 0.1620 | 6-3/4 | 0.407 | 0.407 | 37.0 | 150 |
| S0.61BI | smooth | 11.75 | 11.66 | 10.25 | 10.16 | 2.63 | 0.215 | 3.75 | 31.5 | 0.1620 | 4-1/2 | 1.222 | 0.611 | 33.3 | 203 |
| R0.61BF | rough | 11.81 | 11.56 | 10.31 | 10.06 | 2.62 | 0.217 | 3.75 | 31.5 | 0.1620 | 4-1/2 | 1.222 | 0.611 | 33.3 | 203 |
| S0.92BI | smooth | 11.75 | 11.50 | 10.25 | 10.00 | 2.63 | 0.218 | 4.5 | 30.0 | 0.1620 | 3 | 1.830 | 0.915 | 34.7 | 317 |
| R0.92BF | rough | 11.81 | 11.63 | 10.31 | 10.13 | 2.62 | 0.215 | 4.5 | 30.0 | 0.1620 | 3 | 1.830 | 0.915 | 34.7 | 317 |
| S1.04AI | smooth | 11.81 | 11.69 | 10.31 | 10.19 | 2.62 | 0.214 | 5.44 | 29.125 | 0.1055 | 1-1/8 | 1.037 | 1.037 | 24.3 | 251 |

* See foldout list of symbols after References.

A

| | Prestressing Data | | | | | |
|---|---|---|---|---|---|---|
| | Force (kips) | | | Stresses (ksi) | | |
| ) | $F_{sj}$ | $F_{si}$ | $F_{se}$ | $f_{sj}$ | $f_{si}$ | $f_{se}$ |
| | 15.56 | 15.30 | 14.72 | 143 | 140 | 135 |
| | 15.42 | 14.69 | 13.60 | 141 | 135 | 125 |
| 4 | 13.10 | – | 6.42 | 119 | – | 59 |
| 7 | 15.80 | 15.07 | 14.05 | 145 | 138 | 129 |
| 5 | 15.70 | 14.94 | 14.35 | 144 | 137 | 132 |
| 6 | 15.14 | 14.18 | 13.86 | 139 | 130 | 127 |
| 7 | 15.50 | 15.18 | 14.71 | 142 | 139 | 135 |
| 7 | 15.62 | 14.71 | 14.12 | 143 | 135 | 130 |
| 5 | 15.61 | 15.25 | 14.09 | 143 | 143 | 129 |
| 5 | 15.62 | 14.99 | 14.27 | 143 | 138 | 131 |
| 9 | 15.74 | 15.30 | 14.71 | 145 | 140 | 135 |

B

A

Table 2. Properties of Concrete

| Beam Designation | Beam Section | Aggregate-to-Cement Ratio[a] | Water-to-Cement Ratio[a] | Cement (sack/yd$^3$) | Water (gal/sack) | Slump (in.) | Concrete Strength (psi) | | | |
|---|---|---|---|---|---|---|---|---|---|---|
| | | | | | | | $f'_c$ | | $f_t$ | |
| | | | | | | | Prestressed | Test | Prestressed | Te |
| S0.00I | cast-in-situ | 2.92 | 0.55 | 8.77 | 6.21 | 3.50 | – | 4,930 | – | 51 |
| | precast | 2.96 | 0.55 | 8.62 | 6.21 | 3.25 | 4,530 | 5,600 | 447 | 54 |
| R0.00I | cast-in-situ | 2.90 | 0.56 | 8.77 | 6.32 | 3.0 | – | 5,350 | – | 54 |
| | precast | 2.95 | 0.56 | 8.62 | 6.32 | 2.50 | 4,600 | 5,610 | 433 | 44 |
| S0.26AI | cast-in-situ | 2.82 | 0.54 | 9.00 | 6.09 | 5.50 | – | 5,530 | – | 46 |
| | precast | 2.90 | 0.59 | 9.25 | 6.66 | 3.0 | 3,530 | 5,790 | 389 | 46 |
| S0.39AD | cast-in-situ | 2.83 | 0.55 | 9.00 | 6.21 | 3.0 | – | 4,950 | – | 39 |
| | precast | 2.91 | 0.56 | 8.62 | 6.32 | 4.0 | 3,830 | 5,740 | 411 | 43 |
| S0.39AI | cast-in-situ | 2.92 | 0.54 | 8.77 | 6.10 | 3.25 | – | 5,140 | – | 51 |
| | precast | 2.95 | 0.57 | 8.62 | 6.44 | 3.0 | 3,950 | 5,060 | 395 | 50 |
| S0.41BI | cast-in-situ | 2.83 | 0.54 | 9.00 | 6.10 | 4.0 | – | 4,590 | – | 41 |
| | precast | 2.88 | 0.52 | 9.00 | 5.87 | 4.0 | 4,220 | 5,220 | 417 | 47 |
| S0.61BI | cast-in-situ | 2.95 | 0.55 | 8.62 | 6.21 | – | – | 4,530 | – | 47 |
| | precast | 3.04 | 0.62 | 8.24 | 7.00 | 3.00 | 4,950 | 5,670 | 553 | 54 |
| R0.61BF | cast-in-situ | 2.96 | 0.55 | 8.62 | 6.21 | 2.75 | – | 5,150 | – | 49 |
| | precast | 3.03 | 0.57 | 8.29 | 6.44 | 3.25 | 4,470 | 5,350 | 458 | 50 |
| S0.92BI | cast-in-situ | 2.95 | 0.58 | 8.62 | 6.32 | 3.00 | – | 4,600 | – | 40 |
| | precast | 3.10 | 0.58 | 8.24 | 6.32 | 2.25 | 3,870 | 5,650 | 436 | 46 |
| R0.92BF | cast-in-situ | 3.13 | 0.60 | 8.15 | 6.77 | 2.50 | – | 4,900 | – | 45 |
| | precast | 3.16 | 0.57 | 8.24 | 6.44 | 2.50 | 4,040 | 5,370 | 407 | 43 |
| S1.04AI | cast-in-situ | 2.85 | 0.51 | 9.00 | 5.75 | 2.50 | – | 4,630 | – | 44 |
| | precast | 2.90 | 0.58 | 8.77 | 6.32 | 4.0 | 4,560 | 5,410 | 447 | 55 |

[a] Ratios are by weight and the weight of aggregate is in the saturated surface-dry condition with an absorption capacity of 1%.

B

Table 2. Properties of Concrete

| Aggregate-to-Cement Ratio[a] | Water-to-Cement Ratio[a] | Cement (sack/yd$^3$) | Water (gal/sack) | Slump (in.) | Concrete Strength (psi) | | | | Age (days) | |
|---|---|---|---|---|---|---|---|---|---|---|
| | | | | | $f'_c$ | | $f_t$ | | | |
| | | | | | Prestressed | Test | Prestressed | Test | Prestressed | Test |
| 2.92 | 0.55 | 8.77 | 6.21 | 3.50 | – | 4,930 | – | 511 | – | 8 |
| 2.96 | 0.55 | 8.62 | 6.21 | 3.25 | 4,530 | 5,600 | 447 | 543 | 7 | 15 |
| 2.90 | 0.56 | 8.77 | 6.32 | 3.0 | – | 5,350 | – | 549 | – | 8 |
| 2.95 | 0.56 | 8.62 | 6.32 | 2.50 | 4,600 | 5,610 | 433 | 448 | 8 | 14 |
| 2.82 | 0.54 | 9.00 | 6.09 | 5.50 | – | 5,530 | – | 468 | – | 11 |
| 2.90 | 0.59 | 9.25 | 6.66 | 3.0 | 3,530 | 5,790 | 389 | 464 | 7 | 19 |
| 2.83 | 0.55 | 9.00 | 6.21 | 3.0 | – | 4,950 | – | 395 | – | 9 |
| 2.91 | 0.56 | 8.62 | 6.32 | 4.0 | 3,830 | 5,740 | 411 | 432 | 7 | 16 |
| 2.92 | 0.54 | 8.77 | 6.10 | 3.25 | – | 5,140 | – | 511 | – | 7 |
| 2.95 | 0.57 | 8.62 | 6.44 | 3.0 | 3,950 | 5,060 | 395 | 506 | 7 | 14 |
| 2.83 | 0.54 | 9.00 | 6.10 | 4.0 | – | 4,590 | – | 412 | – | 8 |
| 2.88 | 0.52 | 9.00 | 5.87 | 4.0 | 4,220 | 5,220 | 417 | 470 | 7 | 16 |
| 2.95 | 0.55 | 8.62 | 6.21 | – | – | 4,530 | – | 479 | – | 6 |
| 3.04 | 0.62 | 8.24 | 7.00 | 3.00 | 4,950 | 5,870 | 553 | 546 | 8 | 14 |
| 2.96 | 0.55 | 8.62 | 6.21 | 2.75 | – | 5,150 | – | 490 | – | 7 |
| 3.03 | 0.57 | 8.29 | 6.44 | 3.25 | 4,470 | 5,350 | 458 | 502 | 6 | 13 |
| 2.95 | 0.58 | 8.62 | 6.32 | 3.00 | – | 4,600 | – | 401 | – | 7 |
| 3.10 | 0.58 | 8.24 | 6.32 | 2.25 | 3,870 | 5,650 | 436 | 467 | 6 | 14 |
| 3.13 | 0.60 | 8.15 | 6.77 | 2.50 | – | 4,900 | – | 456 | – | 6 |
| 3.16 | 0.57 | 8.24 | 6.44 | 2.50 | 4,040 | 5,370 | 407 | 435 | 6 | 12 |
| 2.85 | 0.51 | 9.00 | 5.75 | 2.50 | – | 4,630 | – | 446 | – | 8 |
| 2.90 | 0.58 | 8.77 | 6.32 | 4.0 | 4,560 | 5,410 | 447 | 553 | 7 | 18 |

[a] weight of aggregate is in the saturated surface-dry condition with an absorption capacity of 1%.

BLANK PAGE

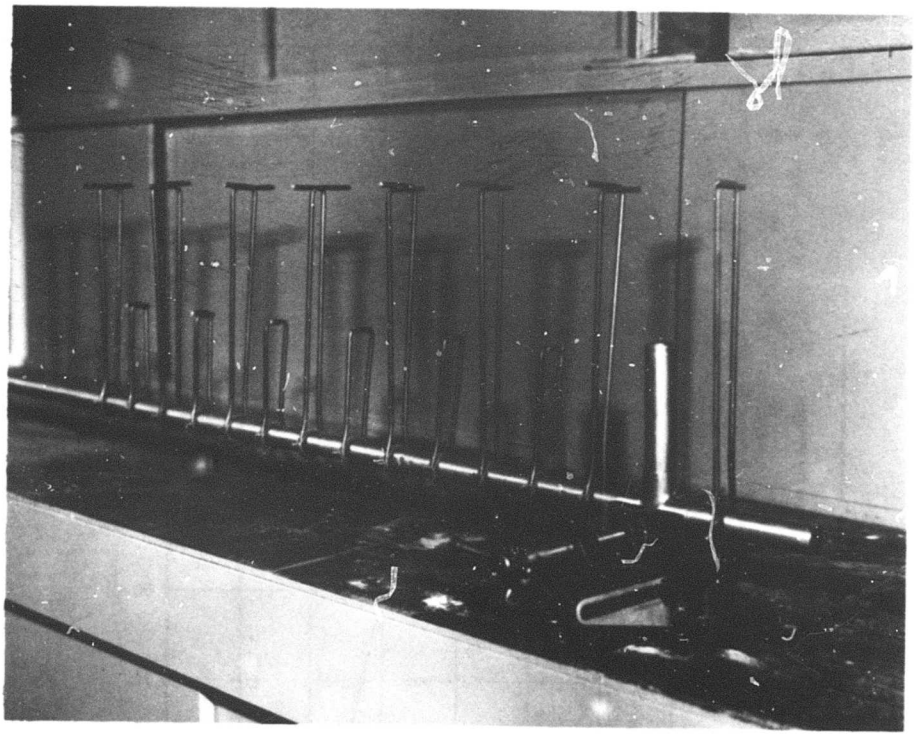

Figure 2. Stirrup cage.

**Grout.** The constituents of grout were Type III portland cement, water, and a water-reducing admixture (Plastocrete). The weight ratio of water to cement was approximately 0.45. The admixture was added in the amount of 5 ounces per 100 pounds of cement.

**Reinforcing Steel.** The prestressing cables used were seven-wire uncoated stress-relieved strands with a 7/16-inch diameter and a 0.109-square-inch area. Tensile tests indicated a stress–strain relationship which was essentially linear up to a stress of 200 ksi with a yield strength of 260 ksi as determined by the 0.2% offset method; the ultimate strength was 303 ksi. A typical stress–strain relationship for the prestressing cable is shown in Figure 4.

Web reinforcement consisted of 12-gage (0.106-inch diameter) and 8-gage (0.162-inch diameter) wires. The yield point for the 12-gage wires varied from 21.0 to 24.3 ksi with an ultimate strength of approximately 42 ksi. The yield point of the 8-gage wire ranged from 33.3 to 37.0 ksi with an ultimate strength of approximately 49 ksi. Values for the yield strength of the stirrups are listed in Table 1. The stress–strain relationships for the web steel exhibited a long yield plateau.

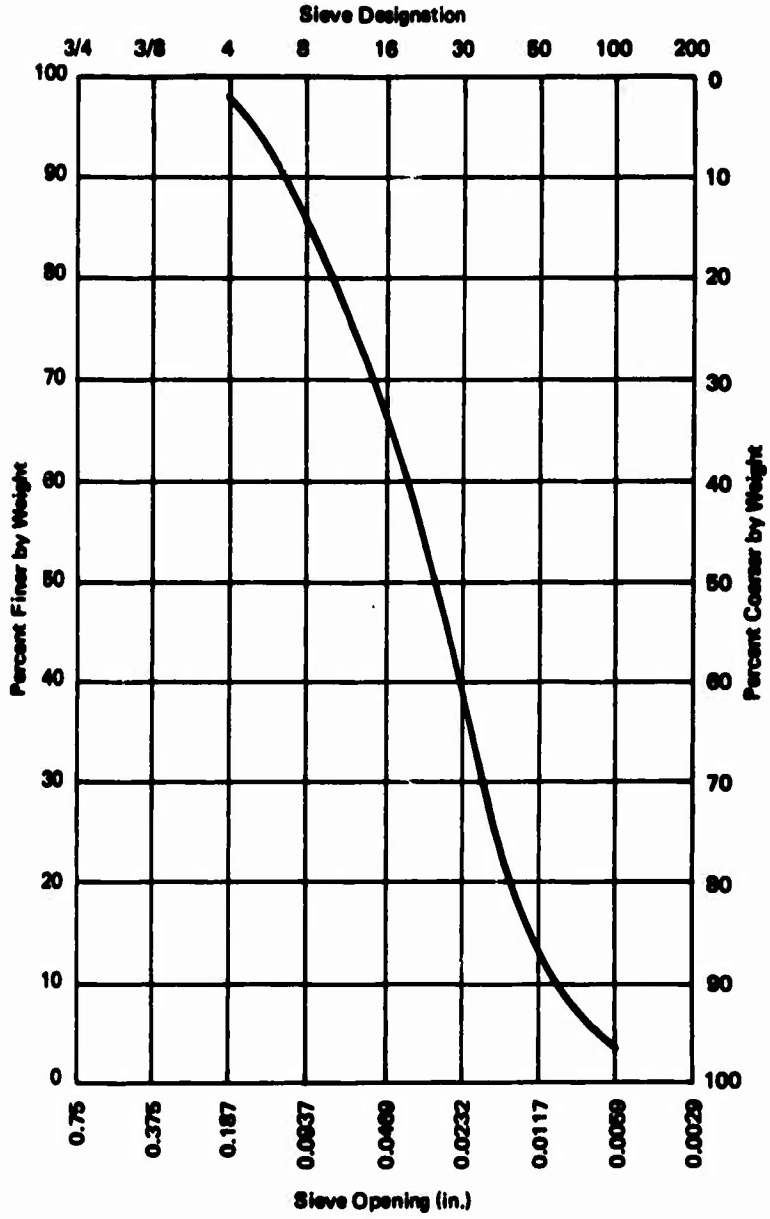


Figure 3. Sieve analysis of aggregate.

## Fabrication

The general evolution routine of each specimen was as follows. A cage was prepared with the appropriate stirrups tied to the rigid conduit. The cage was accurately placed in the forms for the precast element and tied into position for casting. After the precast element was cast, the exposed interface surface was finished to the desired condition of roughness. In order to avoid severe cracking or failure due to handling stresses, the forms were not removed until the concrete was 2 days old. The precast element was cured under wet

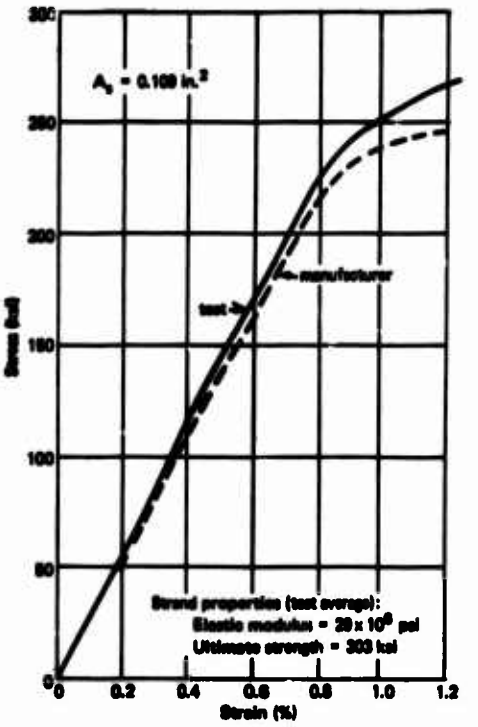


**Figure 4. Tensile stress–strain curves for 7/16-inch seven-wire strand.**

burlap and canvas or polyethylene sheets for approximately 1 week after casting. At this time the precast element was prestressed and the conduit was grouted. Subsequently, the prestressed element was replaced in the forms which were modified for casting the cast-in-situ element. Prestressing and grouting of the precast element and casting of the cast-in-situ element were usually performed on the same day. The composite beam was then allowed to cure under wet burlap for 5 days before drying in the air for instrumentation and testing. Testing of the specimens was performed approximately 2 weeks after casting the precast element and about 1 week after casting the cast-in-situ element. In all cases the control cylinders were subjected to the same curing conditions as the element which they represented.

**Forms.** The forms used to cast the test beams were fabricated from structural steel and wood. Cross sections of the forms are shown in Figure 5. For casting the precast element, the forms consisted of two 6[15.3 sections connected to a 1/4-inch steel baseplate. Wood sections were used to form the outline of the web portion of the precast element. After removal of the precast element from the forms, the wood portions were removed and the channels were reconnected to the 1/4-inch plate. For casting the compression element, two 6[8.2 sections were bolted to the top flange of the 6[15.3 sections. The wood portion of the top channels formed the outline of the cast-in-situ element web. The beam forms as well as the control cylinder molds were cleaned and oiled prior to each casting operation.

**Mixing and Casting.** Concrete was mixed in a 6-cubic-foot-capacity mixer with a nontilting drum. To determine the weight ratios of the mixes presented in Table 2, moisture contents were determined for samples of the sand as it was placed in the mixer. The mixing time was approximately 10 minutes. Each element and its respective control cylinders were prepared from a 6-cubic-foot batch. The slump, as recorded in Table 2, was measured immediately after mixing.

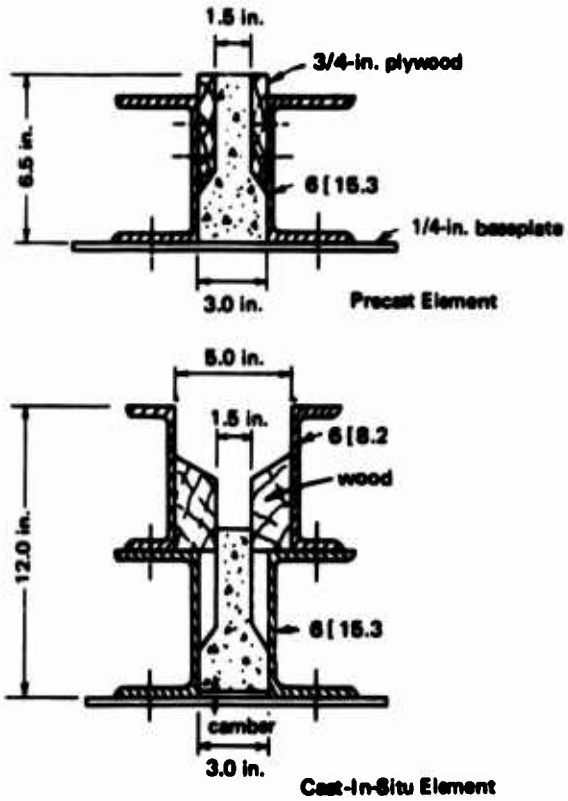


**Figure 5. Forms for casting sections of test beams.**

Twelve 6 x 12-inch control cylinders were cast for each precast element, and six cylinders were cast for the cast-in-situ element. Form vibrators were used to provide continuous vibration for the beams during casting, and internal vibrators were used for the control cylinders.

**Prestressing.** A single prestressing strand was used as the prestressing tendon in the beams. Figure 6 shows the setup for the posttensioning of the precast element.

The prestressing force was distributed over the ends of the prestressed element by 3/4-inch bearing plates. To maintain the prestressing force in the cable, wedge-type grips were attached to the cable outside the load cell at the unjacked end. Another grip was provided between the jack and load cell at the jacking end. The prestressing technique and equipment utilized are outlined in Reference 1.

Immediately before or after the prestressing operation, six control cylinders were tested to evaluate the compressive and the splitting tensile strengths of the concrete.

**Grouting.** After the precast element was prestressed, it was replaced in the forms for casting the cast-in-situ element of the beam. Grout was then forced through the conduit by an air-pressure grout pump. A vertical branch

of the metal conduit located about 6 inches from the end of the beam served as an inlet for the grout, while a similar branch at the opposite end of the beam was the outlet for the air that was displaced by the grout. After the grouting operation, the cast-in-situ element of the beam was cast onto the precast element. Upon completion of the grouting and casting, the prestress force in the cable was measured and recorded.

## Test Equipment and Procedure

**Testing Equipment.** The general loading arrangement is shown in Figure 7. Load was applied to the beam through a system of rockers, steel I-beam, and bearing plates by a hydraulic jack mounted to a rigid loading frame. The force from the jack was measured by a load cell placed between the jack and the rocker sitting on the steel I-beam. The I-beam distributed the jack force equally to two load points on the test beam through rockers and bearing plates. Strain indicators were connected to the jack load cell and to the load cell attached to the prestressing cable. The purpose of the latter load cell was to monitor change in the prestressing cable force.

Slip between the precast and cast-in-situ elements was observed at 10 locations along the interface as shown in Figure 7. The slip gages were cantilevered deflectometers which were constructed from small aluminum beams with strain gages attached to both sides. A typical slip gage is shown in Figure 8. The outputs from the slip gages were channeled through a switching unit and then measured by another strain indicator.

Eight strain gages were also attached to the beam at various locations. In the middle of each shear span, two gages were cemented to the web—one on each side of the interface. To measure flexural strains, four strain gages were cemented at the midspan of the beam. Output from the strain gages were monitored by a strain indicator after being transferred through the switching unit. Deflection was measured by three 0.001-inch dial gages located at the load points and the beam midspan.

All control cylinders were tested in a 400,000-pound-capacity universal testing machine.

**Test Procedure.** The test beam was centered under the loading jack to avoid any difficulties resulting from eccentricity of load. After initial readings were recorded for all gages and load cells, load was incrementally applied. The test usually lasted two hours or more. Load increments were approximately 2,000 pounds before initial cracking and 1,000 pounds afterwards until failure. After each load increment was applied, readings were taken from the strain gages, slip gages, deflection gages, jack load cell, and prestress load cell. The formation of cracking and propagation of existing cracking were noted.

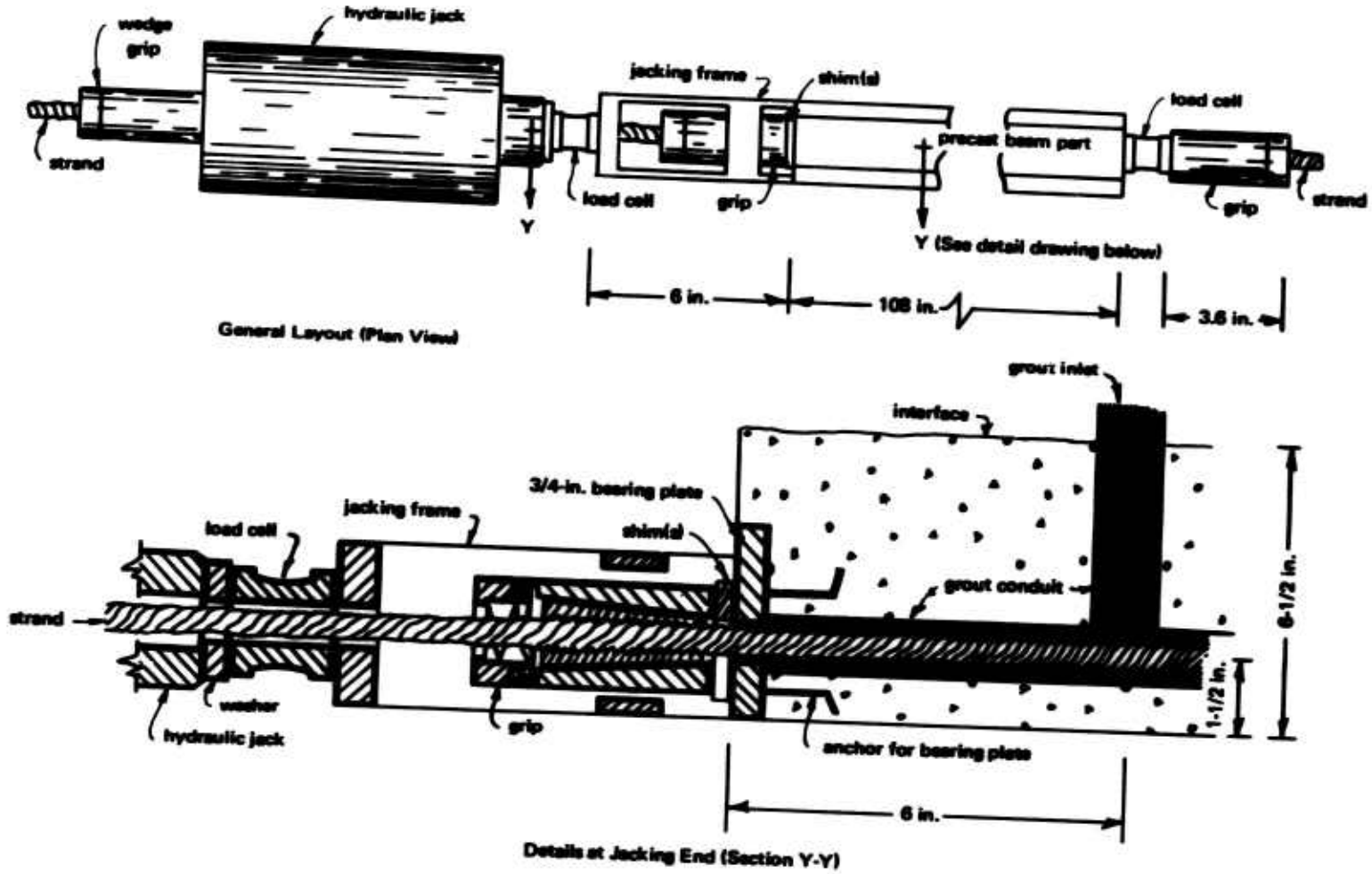


Figure 6. Setup and details for prestressing operation.

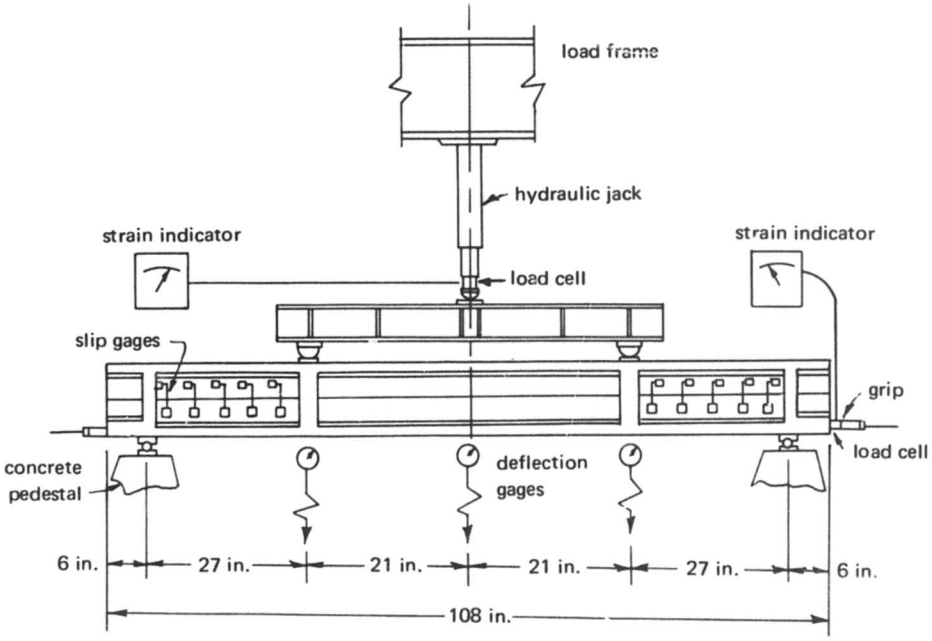


Figure 7. Loading arrangement.

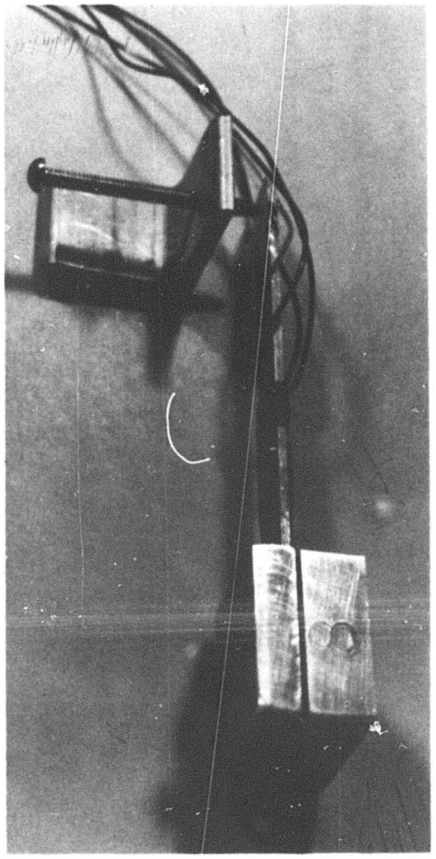

Figure 8. Cantilevered slip gage.

Six control cylinders, three compression tests, and three splitting tensile tests were performed for each element of every beam. The stress rate for the splitting tensile tests was about 110 psi per minute and that for the compression test was approximately 35 psi per second; these rates conform to ASTM C 496-66 and ASTM C 39-66, respectively.

## RESULTS AND DISCUSSION

### General

Values of the measured and computed characteristics of the beams are tabulated in the various tables. Table 3 gives a list of the loads, shears, and deflections measured at initial flexural cracking and at maximum load. Sectional properties of actual beams are recorded in Table 4. Prestress and stirrup data, as well as interface surface conditions for each beam, are given in Table 1.

The concrete compressive and splitting tensile strength of the precast and cast-in-situ elements for each beam are listed in Table 2. The average compressive strength of the precast section at testing was 5,500 psi, while the individual values varied from 5,060 psi to 5,790 psi. The average compressive strength of the cast-in-situ elements was 4,940 psi, with actual values varying between a minimum of 4,530 psi and a maximum of 5,530 psi.

The performance of the beams was compared in terms of load-deflection characteristics, slip traits, shear strengths, and failure modes. The web reinforcement percentage, r, was correlated with the behavioral characteristics of the beams. Failure was classified in accordance with the manner of crack propagation as well as deflection and slip response. Beams S0.39AD, R0.61BF, and R0.92BF failed in modes other than shear transfer across the interface. These beams, therefore, did not fully develop the ultimate interface shear strength at the maximum loading. The shear stress at the maximum load for these beams is expected to represent a lower bound of ultimate interface shear strength.

As was stated earlier, the split-beam specimen was used in order that the interface would be subjected to the maximum shear stress of the section. To determine if the actual cross section of each specimen satisfied that condition, the same "yardstick" was used as in Reference 1. This measure is the ratio of shear stress at the interface, $VQ_i/Ib'$, to that at the centroid of the section, $VQ_m/Ib'$, or, $Q_i/Q_m$. This ratio, which should ideally be unity, was calculated for each specimen and was found to deviate from unity by no more than 0.001. For all practical purposes, the interface was subjected to the maximum shear stress of the cross section.

Table 3. Summary of Results

| Beam | Beam Data | | Test Results | | | | | | Predicted Flexural Resistance, $P_{uf}$[a] (kips) | $\frac{P_u}{P_{uf}}$ | $\frac{w_u}{w_c}$ | Failure Mode |
|---|---|---|---|---|---|---|---|---|---|---|---|---|
| | | | Loads | | Deflections | | Shear Stress | | | | | |
| | $\frac{Q_i}{Q_m}$ | $\frac{Q_i}{Ib'}$ | $P_c$ (kips) | $P_u$ (kips) | $w_c$ (in.) | $w_u$ (in.) | $\frac{VQ_i}{Ib'}$ (psi) | $\frac{V}{b'd}$ (psi) | | | | |
| S0.00I | 0.999 | 0.068 | 10.71 | 14.20 | 0.194 | 0.529 | 482 | 467 | 22.51 | 0.63 | 2.73 | Interface shear |
| R0.00I | 0.999 | 0.068 | 11.90 | 17.58 | 0.193 | 0.780 | 593 | 576 | 22.51 | 0.78 | 4.04 | Interface shear |
| S0.26AI | 0.999 | 0.068 | 8.15 | 13.71 | 0.134 | 0.682 | 460 | 448 | 22.56 | 0.61 | 5.09 | Interface shear |
| S0.39AD | 0.999 | 0.068 | 10.20 | 17.27 | 0.151 | 0.680 | 585 | 566 | 22.55 | 0.77 | 4.51 | Diagonal tension |
| S0.39AI | 0.999 | 0.069 | 10.41 | 16.35 | 0.162 | 0.605 | 553 | 538 | 21.95 | 0.74 | 3.73 | Interface shear |
| S0.41BI | 1.000 | 0.069 | 11.94 | 18.01 | 0.153 | 0.770 | 614 | 594 | 22.16 | 0.81 | 5.03 | Interface shear |
| S0.61BI | 1.000 | 0.068 | 10.36 | 17.26 | 0.171 | 1.180 | 591 | 569 | 22.47 | 0.77 | 6.90 | Interface shear |
| R0.61BF | 0.999 | 0.069 | 11.49 | 25.35 | 0.181 | 1.430 | 851 | 828 | 22.12 | 1.14 | 7.90 | Flexure |
| S0.92BI | 1.000 | 0.070 | 11.23 | 21.90 | 0.160 | 0.994 | 747 | 720 | 22.08 | 0.99 | 6.21 | Interface shear |
| R0.92BF | 0.999 | 0.068 | 10.82 | 24.05 | 0.166 | 1.660 | 810 | 785 | 22.30 | 1.08 | 10.00 | Flexure |
| S1.04AI | 1.000 | 0.068 | 10.99 | 23.35 | 0.137 | 1.280 | 788 | 763 | 22.46 | 1.04 | 9.34 | Interface shear |

[a] Based on full composite action.

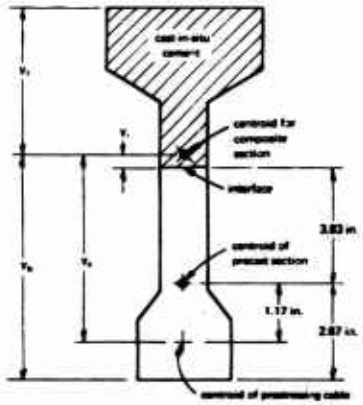


Table 4. Composite Section Properties

| Beam Designation | $E_{ct}$ (psi x $10^6$) | $E_{pt}$ (psi x $10^6$) | Properties of Composite Section at— | | | | | | | | | | | | | | | | | | |
|---|---|---|---|---|---|---|---|---|---|---|---|---|---|---|---|---|---|---|---|---|---|
| | | | Midspan | | | | | | | | | Middle of Shear Span | | | | | | | | | |
| | | | $y_b$ (in.) | $y_s$ (in.) | $y_i$ (in.) | $y_t$ (in.) | A (in.$^2$) | I (in.$^4$) | $r_g$ (in.) | $Q_i$ (in.$^3$) | $Q_m$ (in.$^3$) | $y_b$ (in.) | $y_s$ (in.) | $y_i$ (in.) | $y_t$ (in.) | A (in.$^2$) | I (in.$^4$) | $r_g$ (in.) | $Q_i$ (in.$^3$) | $Q_m$ (in.$^3$) |
| S0.00I | 4.05 | 4.31 | 6.71 | 5.21 | 0.21 | 4.98 | 30.2 | 471.8 | 15.6 | 48.0 | 48.0 | 6.78 | 5.28 | 0.28 | 5.03 | 30.4 | 485.4 | 16.0 | 48.6 | 48.6 |
| R0.00I | 4.21 | 4.32 | 6.78 | 5.28 | 0.28 | 4.91 | 30.8 | 480.7 | 15.6 | 48.7 | 48.8 | 6.86 | 5.36 | 0.36 | 4.95 | 31.0 | 494.5 | 16.0 | 49.3 | 49.4 |
| S0.26AI | 4.28 | 4.38 | 6.79 | 5.29 | 0.29 | 4.90 | 30.8 | 480.4 | 15.6 | 48.7 | 48.7 | 6.91 | 5.41 | 0.41 | 4.97 | 31.1 | 502.3 | 16.2 | 49.6 | 49.8 |
| S0.39AD | 4.05 | 4.37 | 6.69 | 5.19 | 0.19 | 5.00 | 30.0 | 469.1 | 15.6 | 47.7 | 47.8 | 6.81 | 5.31 | 0.31 | 5.00 | 30.2 | 482.6 | 16.0 | 48.4 | 48.4 |
| S0.39AI | 4.13 | 4.09 | 6.72 | 5.22 | 0.22 | 4.81 | 31.2 | 471.2 | 15.1 | 48.6 | 48.7 | 6.89 | 5.39 | 0.39 | 4.89 | 31.5 | 500.1 | 15.9 | 49.9 | 50.1 |
| S0.41BI | 3.90 | 4.16 | 6.63 | 5.13 | 0.13 | 4.96 | 30.1 | 461.7 | 15.3 | 47.6 | 47.6 | 6.73 | 5.23 | 0.23 | 5.02 | 30.1 | 479.6 | 15.8 | 48.4 | 48.4 |
| S0.61BI | 3.88 | 4.34 | 6.60 | 5.10 | 0.10 | 5.06 | 29.4 | 457.6 | 15.6 | 46.9 | 46.9 | 6.65 | 5.15 | 0.15 | 5.10 | 29.5 | 467.4 | 15.8 | 47.3 | 47.3 |
| R0.61BF | 4.13 | 4.21 | 6.70 | 5.20 | 0.20 | 4.86 | 30.7 | 467.8 | 15.2 | 48.2 | 48.2 | 6.86 | 5.36 | 0.36 | 4.95 | 31.1 | 496.4 | 15.9 | 49.5 | 49.6 |
| S0.92BI | 3.91 | 4.33 | 6.51 | 5.01 | 0.01 | 4.99 | 29.3 | 442.5 | 15.1 | 46.2 | 46.2 | 6.67 | 5.17 | 0.67 | 5.08 | 29.7 | 469.6 | 15.8 | 47.5 | 47.6 |
| R0.92BF | 4.03 | 4.22 | 6.70 | 5.20 | 0.20 | 4.93 | 30.4 | 469.8 | 15.4 | 48.1 | 48.1 | 6.82 | 5.32 | 0.82 | 4.99 | 30.7 | 490.2 | 16.0 | 49.0 | 49.1 |
| S1.04AI | 3.92 | 4.24 | 6.67 | 5.17 | 0.17 | 5.02 | 30.0 | 469.2 | 15.6 | 47.8 | 47.8 | 6.65 | 5.15 | 0.15 | 5.16 | 30.2 | 482.7 | 16.0 | 48.4 | 48.4 |

In addition to the slip gages, strain gages were cemented at midshear span on each side of the interface. The measurements from these gages were to be utilized to determine the loading at which the beams began deviation from monolithic behavior. Because of cracking in the region of the gages, the results from them were generally inconclusive in determining impending separation of the beam elements and are not presented.

**Beam Behavior and Mode of Failure**

Initial behavior of the test beams was similar regardless of the variables considered. Typically, output from the concrete strain gages and deflection were almost linearly related to load within 80% to 90% of the initial flexural cracking load. The slip gages indicated slight relative movement between the two beam elements.

Initial cracking consisted of one or more flexural cracks usually forming near the load points. Further loading resulted in the extension of these cracks upward and the formation of additional flexural cracks within the constant-moment region. The flexural cracks proceeded to at least the height of the interface and into the cast-in-situ element before any cracks were formed within the shear span. Initial cracking within the shear span was usually in the form of a small localized diagonal tension crack in the web of the cast-in-situ element near one of the load points. Cracking along the interface of the two elements was next to form. The extent of interface cracking varied from beam to beam depending upon the interface conditions and the stirrup parameter.

**Smooth Interface Surfaces.** Except for S0.39AD, all the beams with smooth interfaces failed as a result of insufficient shear strength along the interface. Beam S0.39AD failed because of diagonal tension. It is interesting to note that all the smooth interface beams except S0.39AD and S0.001 failed at the unjacked end. Typical crack patterns for horizontal shear failures are shown in Figures 9 and 10.

After formation of the small diagonal crack in the web of the cast-in-situ element, a horizontal crack propagated from it along the interface toward the neighboring support. For beams with r of 0.41% or less, the propagation of horizontal cracking along the interface was rapid and failure followed instantly or within one load increment. These beams provided little warning of impending failure, since cracking prior to failure was minimal and the midspan deflection was only 0.45 to 0.50% of the beam length before failure. In beams with r of 0.61% or greater, three or more small localized diagonal cracks formed within the shear span in the web of the cast-in-situ element before horizontal

interface cracking was observed. One or more of these cracks were observed to cross the interface and extend into the precast element. The interface cracking always initiated from diagonal cracks whether or not they crossed the interface. The interface cracking progressed with subsequent load increments. Failure was not as sudden as for beams with smaller **r**. The midspan deflection at failure of the beams with **r** of 0.61% or greater varied from 0.8 to 1.1% of the beam length.

NOT REPRODUCIBLE

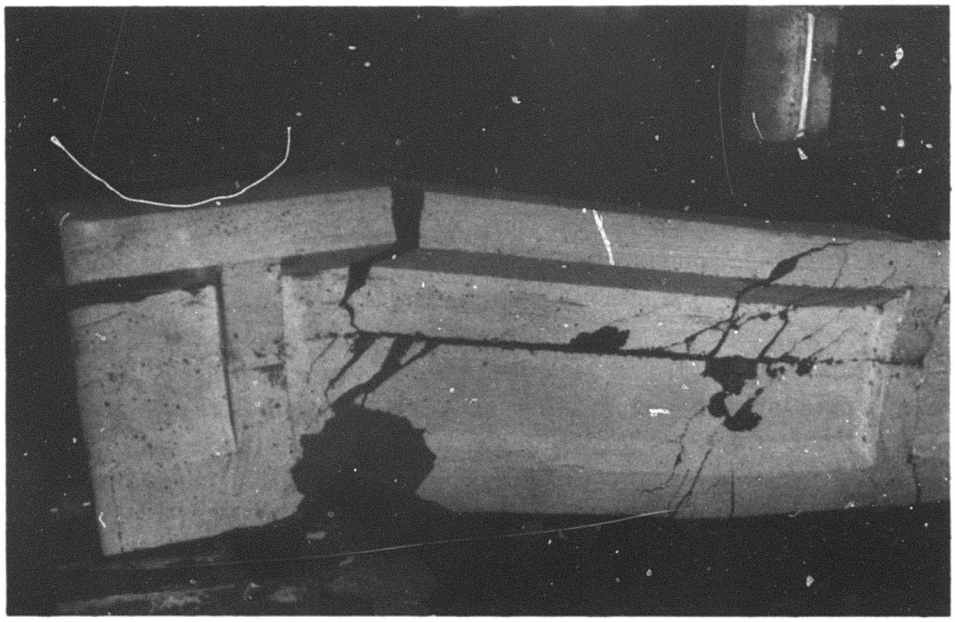

**Figure 9. Interface shear failure of beam S1.04AI with 12-gage stirrups.**

The horizontal cracks along the interface and the slippage between the two beam elements usually lead to the development of a vertical "relief" crack within 8 inches from the support. This crack started at the top surface of the cast-in-situ element and propagated downward through the web. It usually formed immediately before or simultaneously with the maximum load. By the time the relief crack had formed, the cast-in-situ element was almost ineffective in resisting the applied loading. As a result, the precast element had to carry the entire load; the bottom flange of the beam eventually crushed near the support (Figures 9 and 10).

An increase in stirrup area provided an increase in the margin of load-carrying capacity between the load at which horizontal cracking occurred along the interface and the maximum load. For instance, the interface cracking was visible along the shear span of beam S0.92BI at 92% of maximum load compared to the occurrence of interface cracking simultaneously with failure in beams having **r** equal to or less than 0.39%.

NOT REPRODUCIBLE

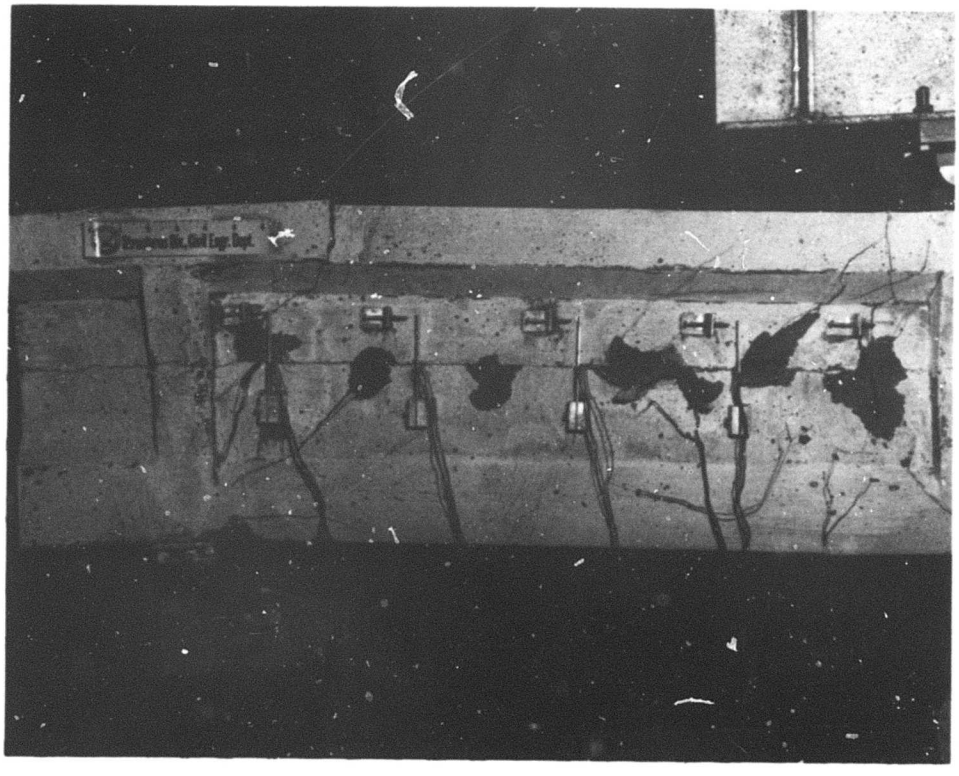

**Figure 10. Interface shear failure of beam S0.61BI with 8-gage stirrups.**

After maximum loading was reached, there was a definite and sudden load drop for the beams with few or no stirrups across the interface. For instance in beam S0.39AI, the load drop at maximum loading was 35% of the maximum value. However, in beams with higher values of **r**, such as beam S1.04AI, there was a "leveling off" of the beam's resistance after attaining maximum load. At this stage of loading, excess slip resulted in shearing of the stirrups when 12-gage wire was used (Figure 9) and caused spalling of the concrete around the stirrups when 8-gage wire was used (Figure 10).

**Rough Interface Surface.** The localized diagonal tension cracks formed in the web of the cast-in-situ element as in the beams with smooth interfaces. However, instead of traveling along the interface for any length greater than 3 inches, they extended diagonally into the web of the precast element.

At ultimate load of R0.61BF and R0.92BF, the flange of the constant-moment region of the beam severely crushed, resulting in the complete collapse of the beams. A photograph of the crack pattern of the jacked-end shear span of beam R0.92BF at the ultimate load is shown in Figure 11. The relief crack did not form in the cast-in-situ element flange of these beams.

NOT REPRODUCIBLE

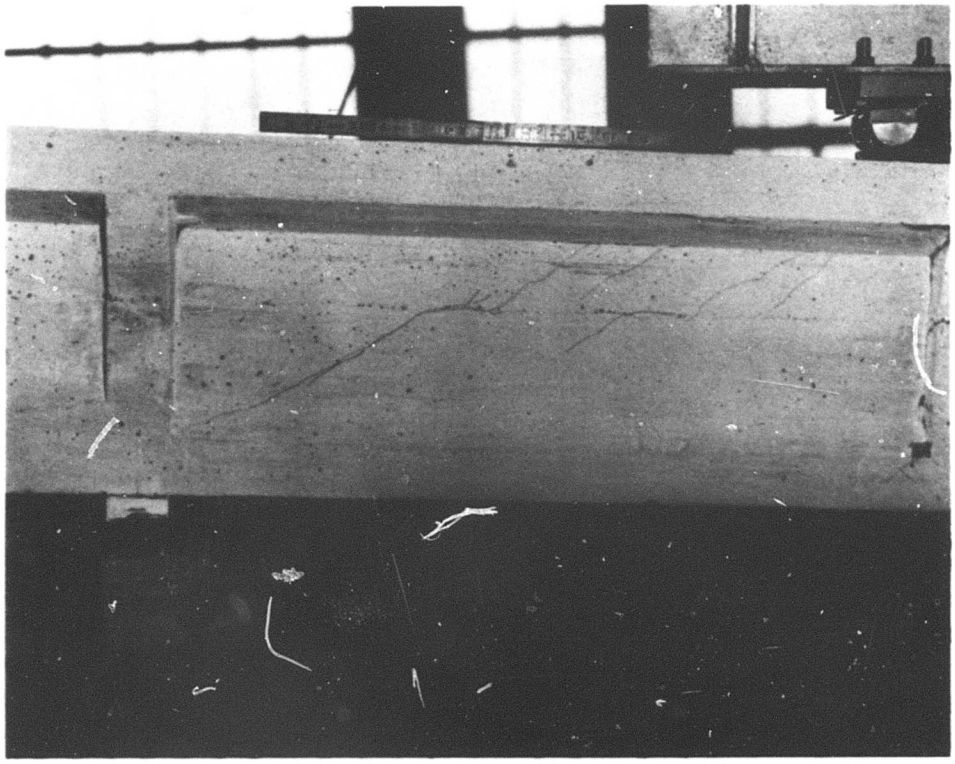

Figure 11. Shear span crack pattern of beam R0.92BF after flexural failure.

Beam R0.00I failed by separation at the interface of the jacked-end shear span after the formation of a large diagonal crack across the interface at mid-shear span. Simultaneously with interface separation, a relief crack was formed in the flange of the cast-in-situ element. At failure, the load dropped to approximately zero in all beams with rough interfaces.

**Prestressing-Cable Force.** Before ultimate load there was usually an erratic increase in the prestressing force due to breakdown in bond. As was stated earlier, the prestressing force was monitored at the unjacked end. For those beams which failed at the unjacked end with less than 20 kips of applied load, the prestressing force usually increased 2 kips or less at maximum load. However, the prestressing-cable force of beam R0.00I, which failed at the jacked end, decreased 1/2 kip at maximum load. In the other two beams that failed at the jacked end, S0.00I and S0.39AD, the prestressing force increased 2 kips at maximum load. For applied load in excess of 20 kips, the rate of change in the prestressing force increased. The force in the cable of beam S0.92BI increased 7 kips at maximum load, while that of beams S1.04AI, R0.61BF, and R0.92BF increased by more than 10 kips.

## Deflection

The load—deflection curves for all beams are plotted in Figure 12. The deflections were taken from the gages located at the midspan of the beam. Up to the flexural cracking load, the load—deflection behavior exhibited by the various test beams was similar regardless of the degree of interface roughness and the amount of web reinforcement across the interface. Initial load—deflection slope ranged from 66.7 to 76.9 kip/in. without any trend corresponding to interface roughness or r. Beyond the flexural cracking load, increased web reinforcement crossing the interface enabled the beams to sustain higher loads and greater deflections, which produced greater toughness and the more desirable ductile failure.

The ratio of deflection at maximum load to that at initial flexural cracking, $w_u/w_c$, was used as a measure of ductility. Plotted in Figure 13 is a curve showing the relationship between this deflection ratio and the web reinforcement ratio. The deflection ratio increased as r was increased; the interface roughness also appeared to increase $w_u/w_c$.

In addition to the midspan deflection gage, a gage was also placed at each load point. Until interface separation became more prominent in one shear span, the observed deflections from these gages indicated the symmetry of the beam-deflection pattern. When the measured slip had reached 0.002 inch or more, a differential between the deflections measured at the load points was detected. For beams with r of 0.61% or less, the difference between the deflections at each load point was very slight before maximum load.

## Ultimate Strength and Interface Shear Stress

Interface roughness and quantity of web steel across the interface improved the integrity and strength of the interface. The ratio of the measured resistance at failure to the predicted flexural resistance was correlated to the amount of web reinforcement crossing the interface. Values of $P_u/P_{uf}$ are tabulated in Table 3 and plotted against r in Figure 14. Because of the increased shear capacity of the interface, beams R0.92BF and S1.04AI were able to develop the predicted flexural capacity. Beams R0.92BF and R0.61BF failed in flexure, while S1.04AI failed by interface separation at a load approximately equal to the predicted ultimate flexural load. For smooth interfaces, values of $P_u/P_{uf}$ varied from 0.61 for beam S0.26AI to 1.04 for beam S1.04AI; for rough interfaces, this resistance ratio ranged from 0.78 for R0.00I to 1.14 for R0.61BF.

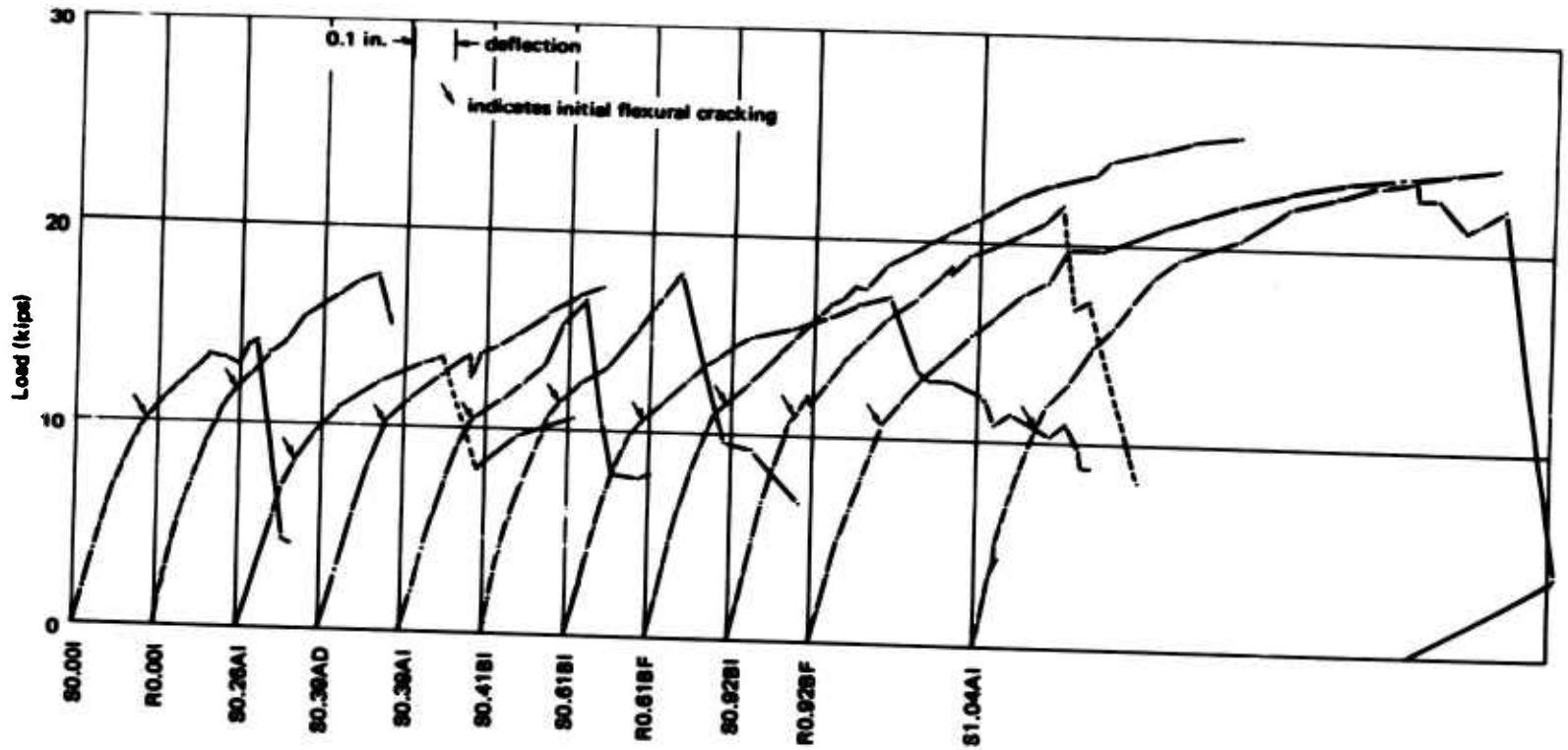


Figure 12. Load–deflection response.

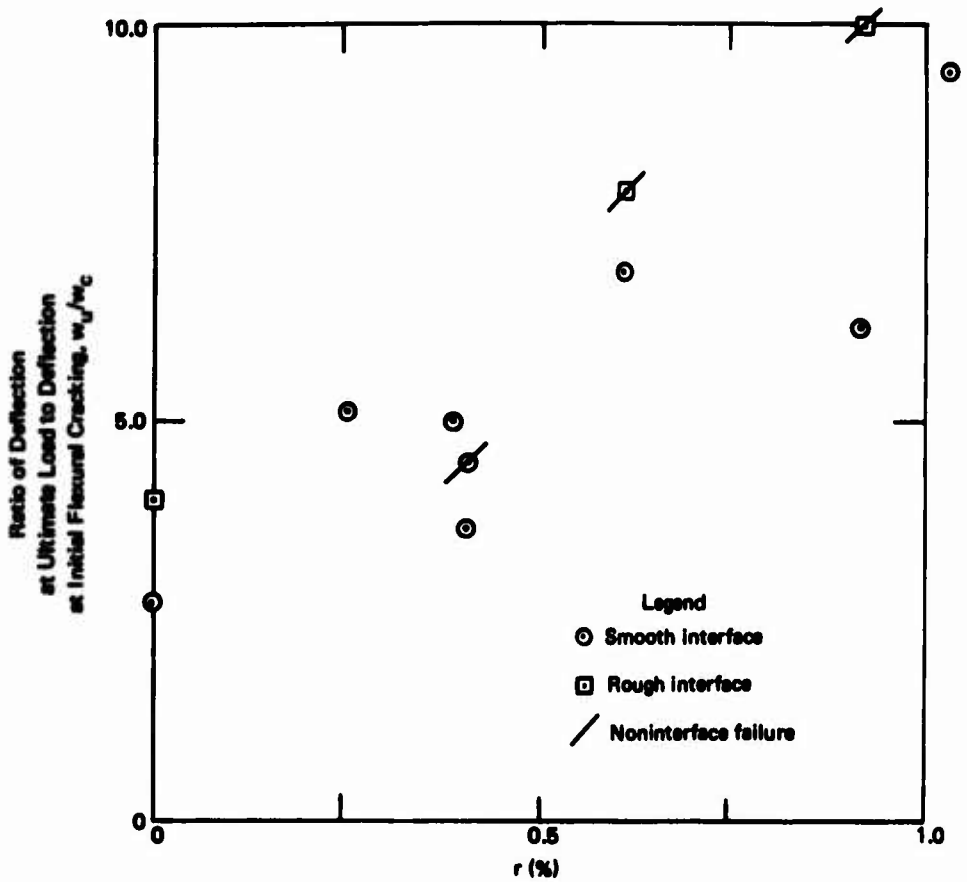


**Figure 13. Ratio of midspan deflection at ultimate load to midspan deflection at initial flexural cracking.**

The interface shear stresses at maximum load were calculated using the standard relationship $v_h = VQ_t/Ib'$. Although this expression does not represent the actual stress conditions, particularly after discontinuities have occurred because of cracking and slip, the calculated stress provides a common basis for comparison. The value of $Q_t/Ib'$ (Table 3) was based on the gross transformed section at the middle of the shear span. For beams with smooth interfaces, the interface shear strength ranged from 460 psi (beam S0.26AI) to 788 psi (beam S1.04AI). For S0.00I, which had a smooth interface and no stirrups crossing the interface, an ultimate shear strength of 482 psi was attained as compared with 593 psi for R0.00I, a similar beam with a roughened interface. A maximum interface shear stress of 851 psi was resisted by R0.61BF before the beam failed in flexure. In general, beams with rough interfaces developed at least 100 psi greater shear strength than beams with equal web reinforcement and smooth interface surface.

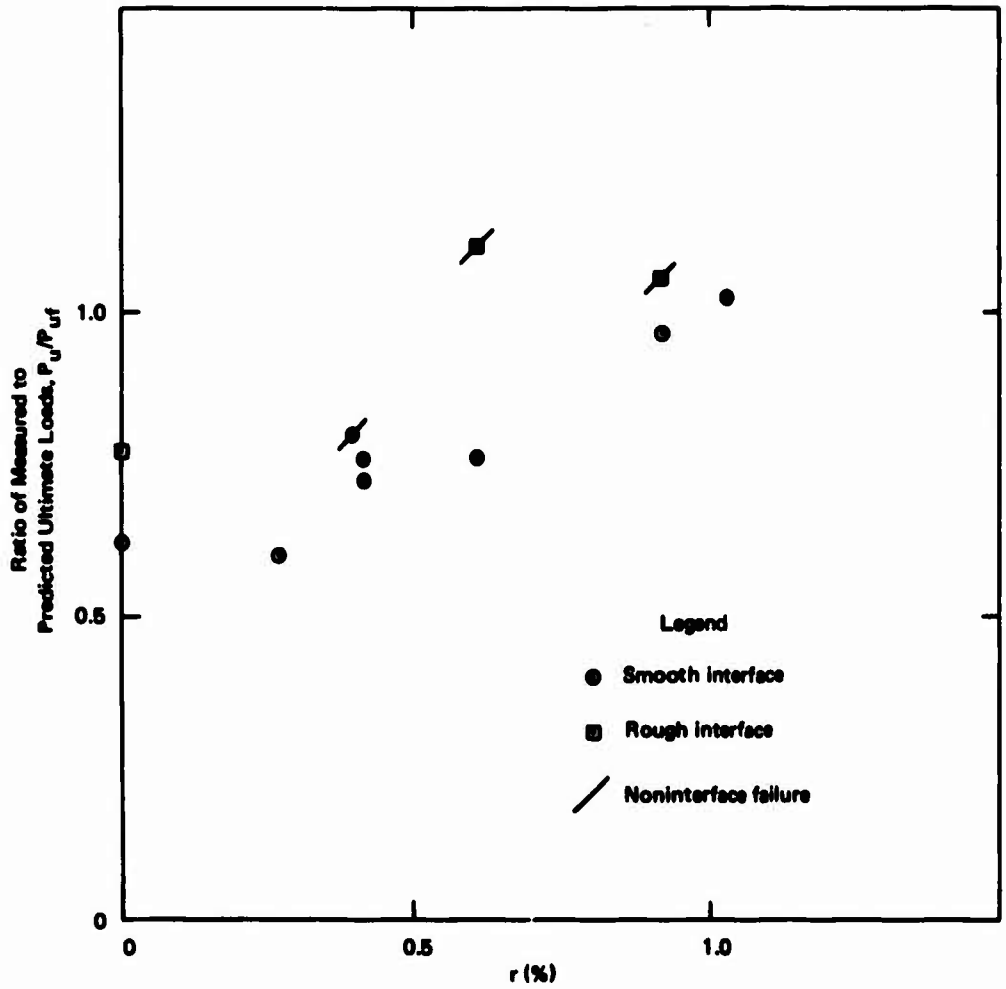


**Figure 14. Ratio of measured ultimate load to predicted flexural resistance.**

The plots in Figures 15 and 16 illustrate the relationship of maximum shear stress to r and $rf_y$, respectively. Also plotted for comparison are graphs of expressions for ultimate horizontal shear strength which were obtained from previous studies.[4-6] In general, the various expressions predict conservative values for the interface shear strength of the specimens.

The expression

$$v_h = \frac{2{,}700}{(a/d) + 5} + 300r\,\frac{33 - (a/d)}{(a/d)^2 + 6(a/d) + 5}$$

(presented in Reference 4) best portrays the trend indicated by the tests (Figure 15). This expression was proposed for both rough and smooth interfaces in reinforced concrete and considers interface shear strength as a function of the web reinforcement ratio as well as the ratio of shear span to effective depth. However, all the experimental values fall above the curve.

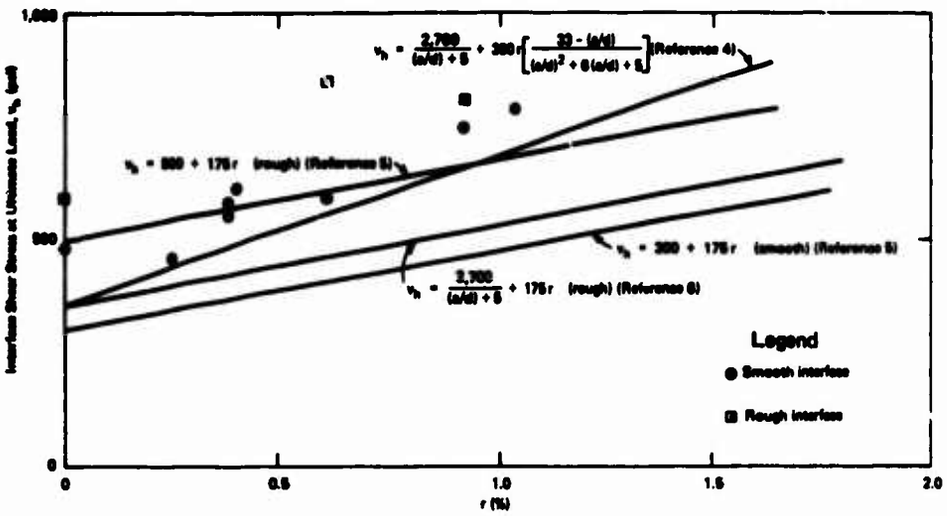


Figure 15. Relationship between interface shear stress and percentage of web reinforcement.

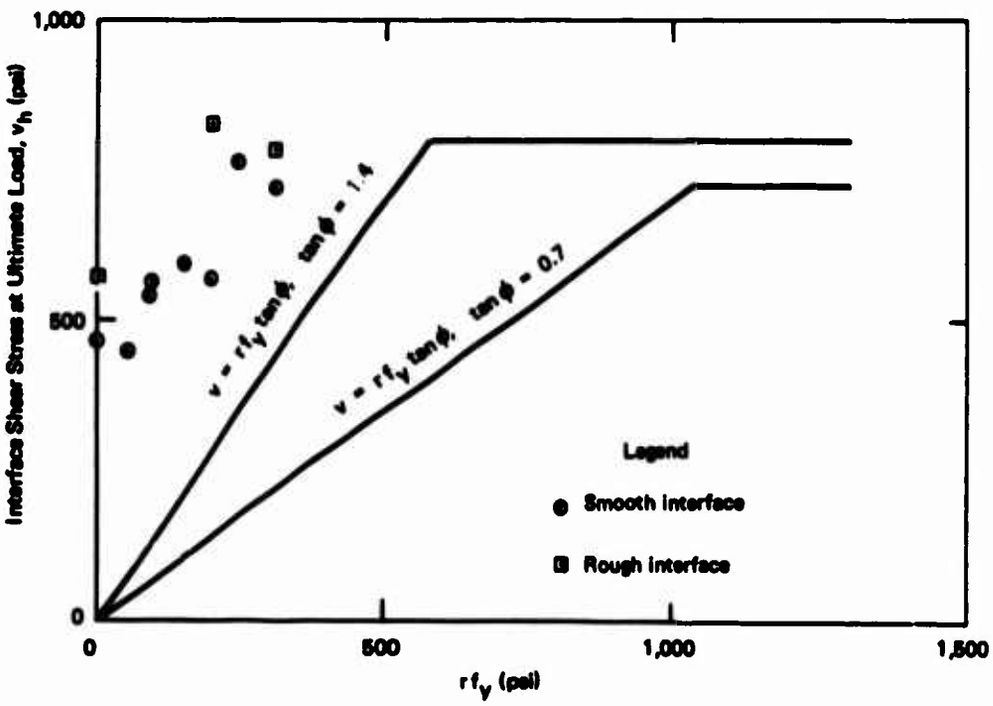


Figure 16. Relationship between interface shear stress and $rf_y$.

The graphs plotted in Figure 16 represent the "shear friction" hypothesis (References 7 and 8), which has been incorporated into the American Concrete Institute (ACI) building code.[9] Figure 17 is a plot of the experimental values of V/b'd against ACI code values. Obviously the code allowances are conservative.

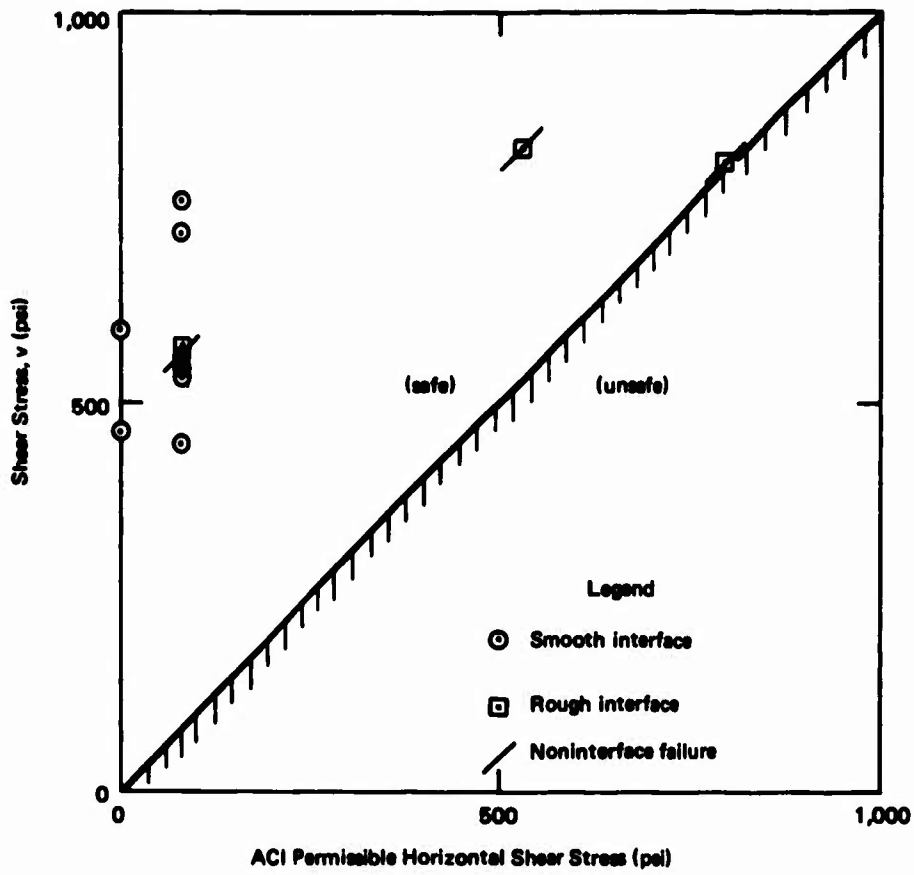


Figure 17. Comparison of observed and recommended shear stress.

The results were compared with experimental values reported in References 1 and 10. These references discuss prestressed composite beams which were reported to have failed because of interface shear. The study[10] utilized a T-beam with a prestressed precast stem and a lightweight-concrete cast-in-situ flange with a/d equal to 3.77. The interface was an exposed aggregate surface. As stated earlier, the specimen used in Reference 1 was a split beam similar to the one used in the present investigation but with a smaller cross section and an a/d equal to 3.68. The experimental shear stress values from all three investigations are plotted against r in Figure 18. Although the trends are similar, the shear strengths are higher for the lower values of a/d. The increase indicates the effect of the load and reaction confinement, which is more predominant with a small value of a/d.

It is interesting to note the apparent lack of effect of stirrup spacing in the interface shear resistance. For specimens S0.39AI and S0.41BI as well as S0.92BI and S1.04AI, the value of r is approximately equal for each pair,

while the spacing of the 12-gage stirrups is less than half of that for the 8-gage. Noting the interface shear strengths of these specimens in Table 3, it would appear that the stirrup spacing had little effect on the shear strength. However, for crack arresting and minimizing stress concentrations, stirrups are expected to be more effective in increasing interface shear strength if their area is distributed evenly in the shear span. For more extreme cases than those covered by the tests, it would seem likely that, for the same r, large stirrups with large spacing would be less effective than smaller stirrups more closely distributed. That is, there would be a limiting value on the spacing similar to recommendations used for web reinforcement based on diagonal tension. The establishment of this limitation should receive attention in future studies.

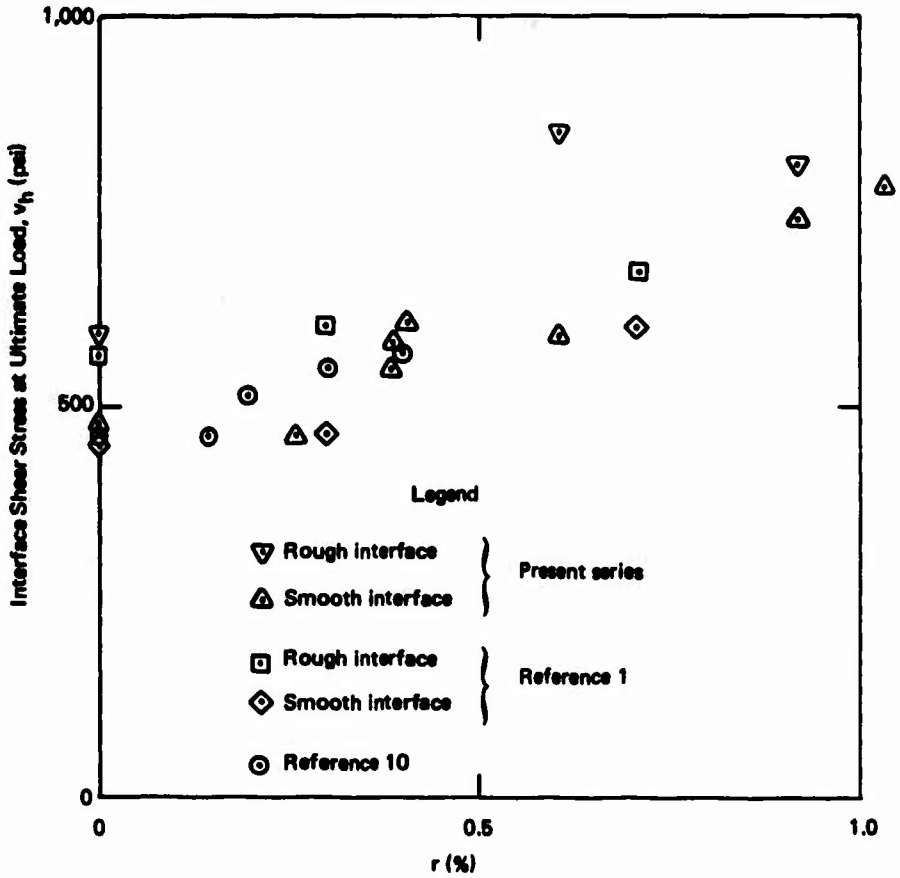


Figure 18. Comparison with other data.

## Slip

Slip initiated usually between midshear span and load points. Initial slip was recorded after interface shear stresses exceeded 300 psi. This corresponded to a loading of approximately 90% of the flexural cracking load.

For loading less than approximately 80% of maximum load, the distribution as well as the magnitude of slip in the shear spans of each beam was similar. For beams with r less than 0.39%, the distribution of slip was similar right up to maximum load. A plot of the slip distribution with certain loads at various locations along the beam is presented in Figure 19. The slip measured at points between the midshear span and the load point was usually predominantly higher than the recorded slip at other locations. Slip recorded from the gages at these "critical" locations were used in the slip plots presented in Figures 20 through 24.

Shown in Figure 20 are load—slip curves for all test beams. In Figure 21 plots are presented of shear stress versus r at slips of less than 0.0001 inch (Figure 21a), 0.0005 inch (Figure 21b), 0.001 inch (Figure 21c), and 0.003 inch (Figure 21d). The effect of increasing the amount of reinforcement across the interface and the interface roughness on shear stress is shown in Figure 21. At slips less than 0.0005 inch, the interface shear stress did not vary with r; however, at slips of 0.001 inch and 0.003 inch, shear stress was increased with r and with interface roughness. It was inferred that the rate of slip decreased with an increase in r and from smooth to rough interface surfaces. After initiation, slip occurred at a rate of 0.0025 to 0.0035 in./ksi of interface shear stress in beams with smooth interfaces and at a slower rate, 0.002 to 0.0025 in./ksi, for beams with roughened interfaces. The higher slip rates were associated with lower values of r. A general value of 0.0025 in./ksi was noted from Reference 1.

At a slip which varied from 0.0005 to 0.0008 inch for smooth interfaces and equaled about 0.0011 inch for rough interfaces, the rate of slip increased from its initial value (Figure 22). This corresponded to an interface shear stress of about 400 to 550 psi for smooth interfaces and 500 to 600 psi for rough interfaces (Figure 23). For beams with $r < 0.39\%$, failure quickly followed, while beams with $r > 0.41\%$ continued to carry increasing load but at an increased slip rate of 0.07 to 0.16 in./ksi of interface shear stress.

Shown in Figure 24 is a plot of the interface shear stress versus slip at 96 to 100% of maximum load. It usually was not possible to obtain the slip distribution right at maximum load. From Figure 24 it can be inferred that failure at 400-psi interface shear should be precluded by little or no slip and that as interface shear strength is increased slip at failure is increased with shear stress. Beams with $r < 0.39\%$ failed at a slip from 0.001 to 0.002 inch, while beams with higher r exhibited greater slips at maximum load. For example, beam S1.04AI failed when the slip reached 0.015 inch. Increased web reinforcement across the interface decreased the likelihood of a sudden separation of the beam elements and increased the energy-absorption capacity of the interface.

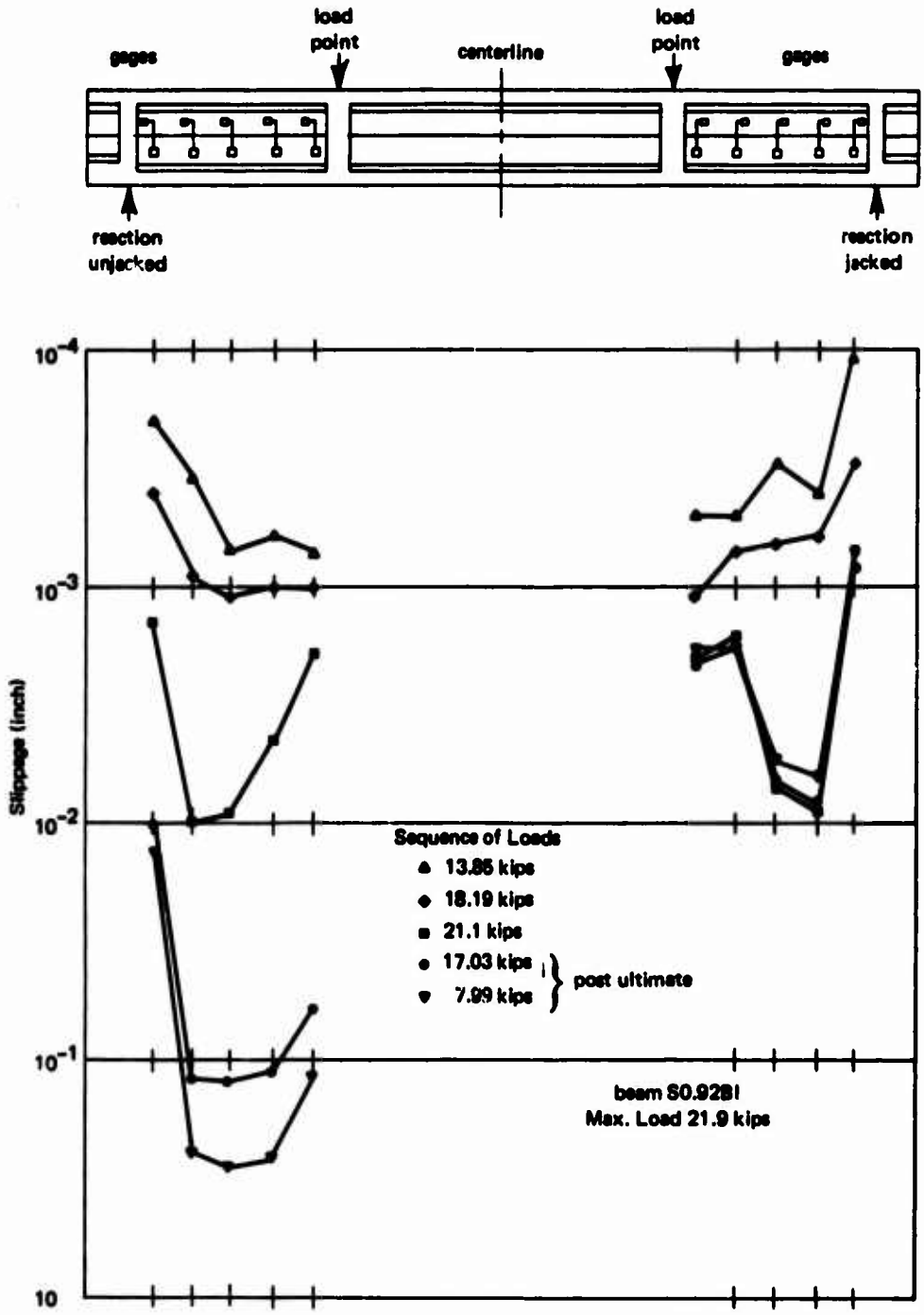


Figure 19. Slip distribution.

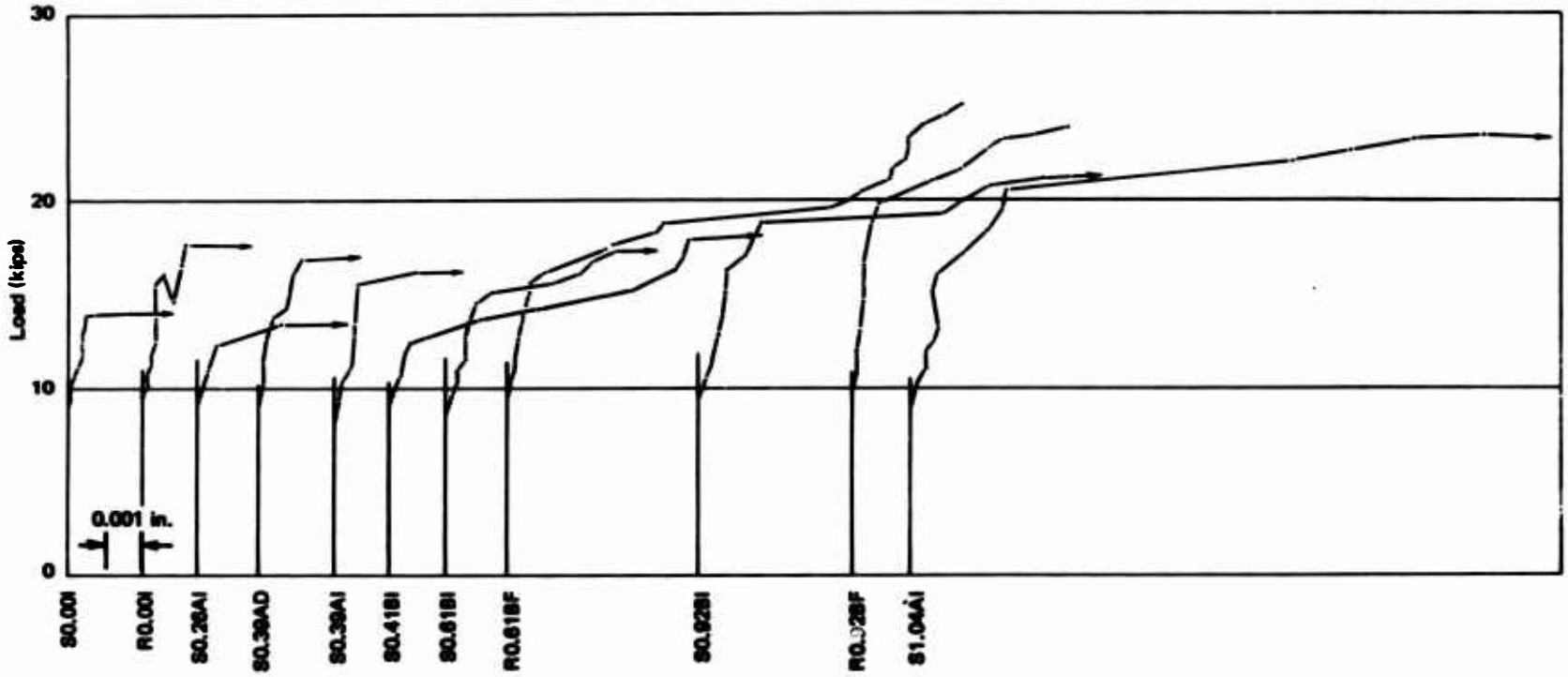


Figure 20. Maximum slip response.

A

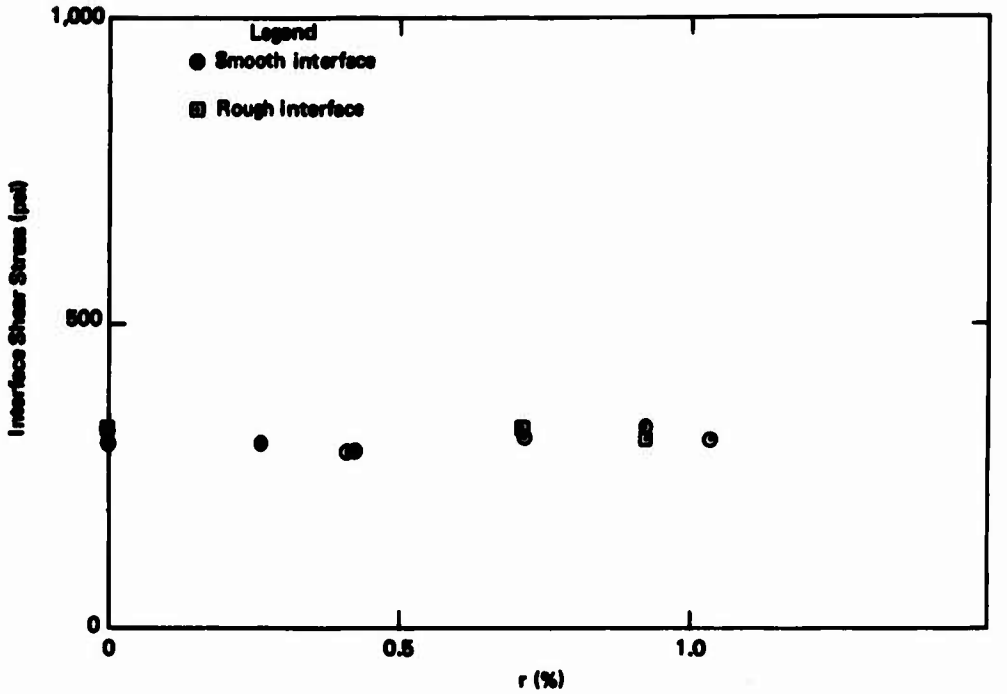


(a) At slip initiation.

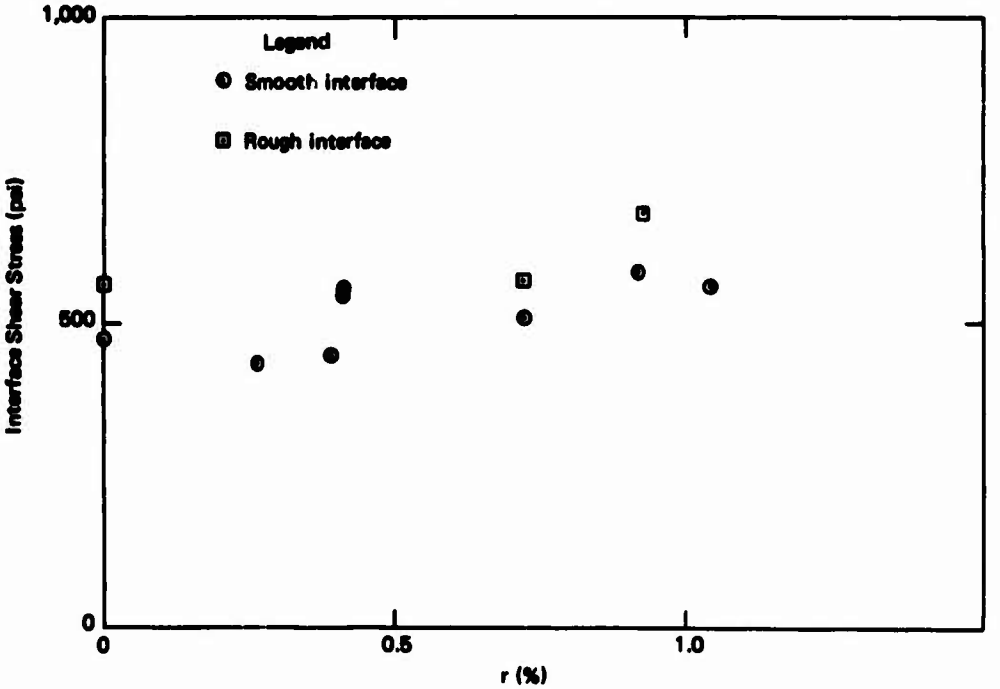


(c) At 0.001-inch slip.

Figure 21. 1

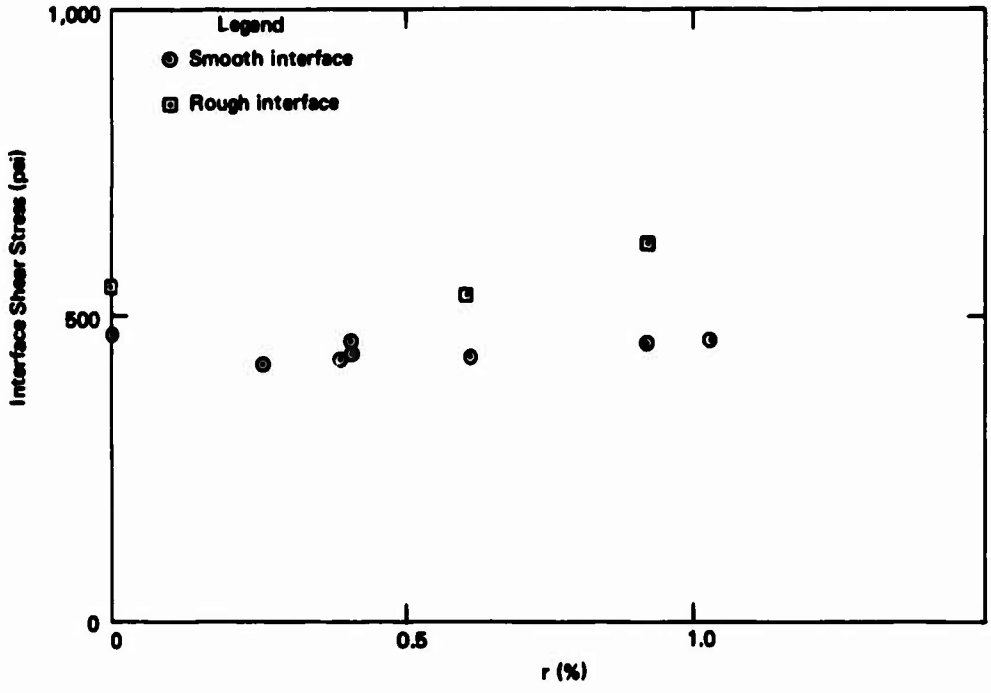


(b) At 0.0005-inch slip.

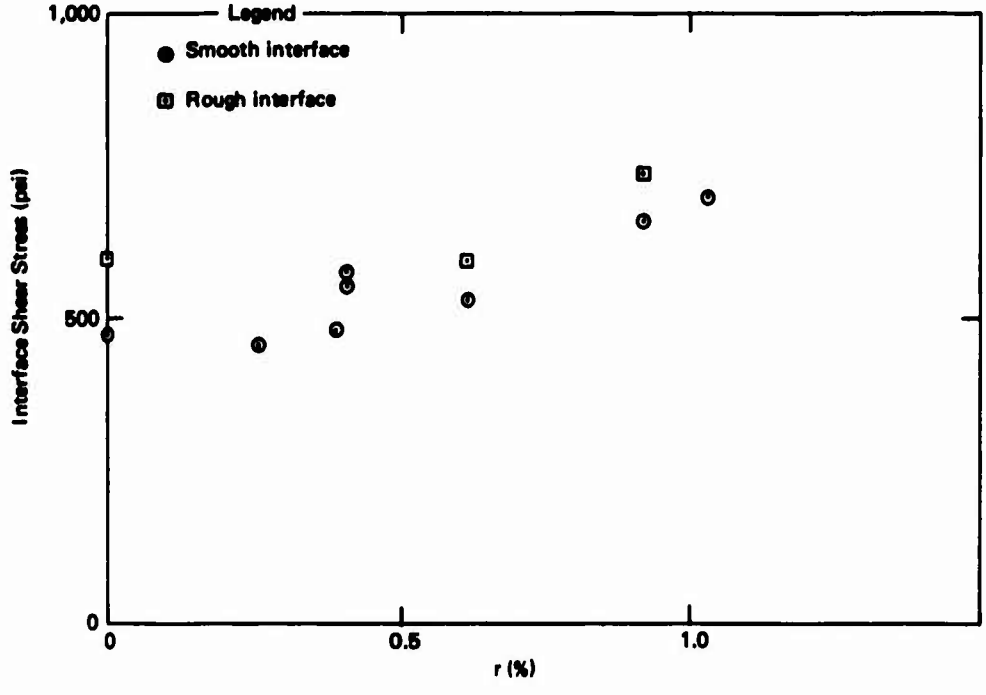


(d) At 0.003-inch slip.

nterface shear stress.

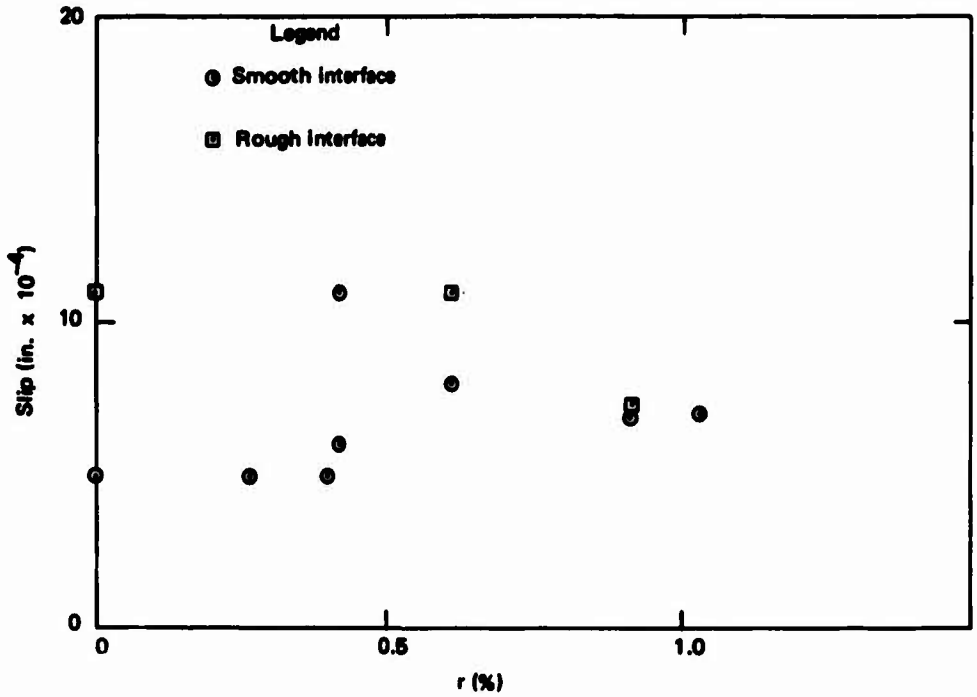


Figure 22. Slip at change of slip rate.

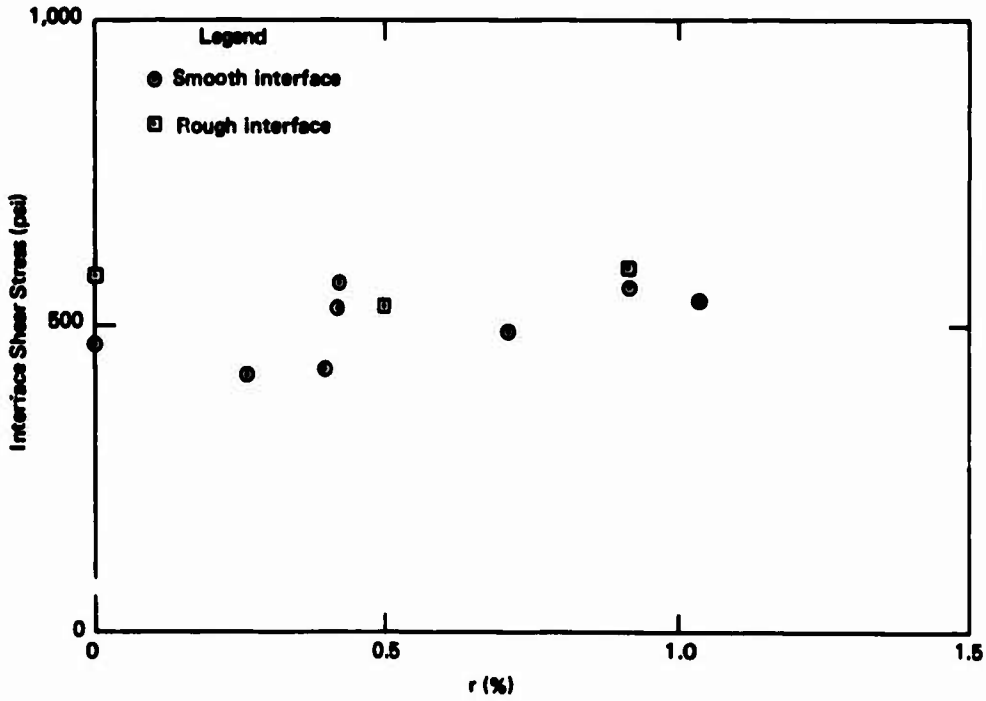


Figure 23. Shear stress at change of slip rate.

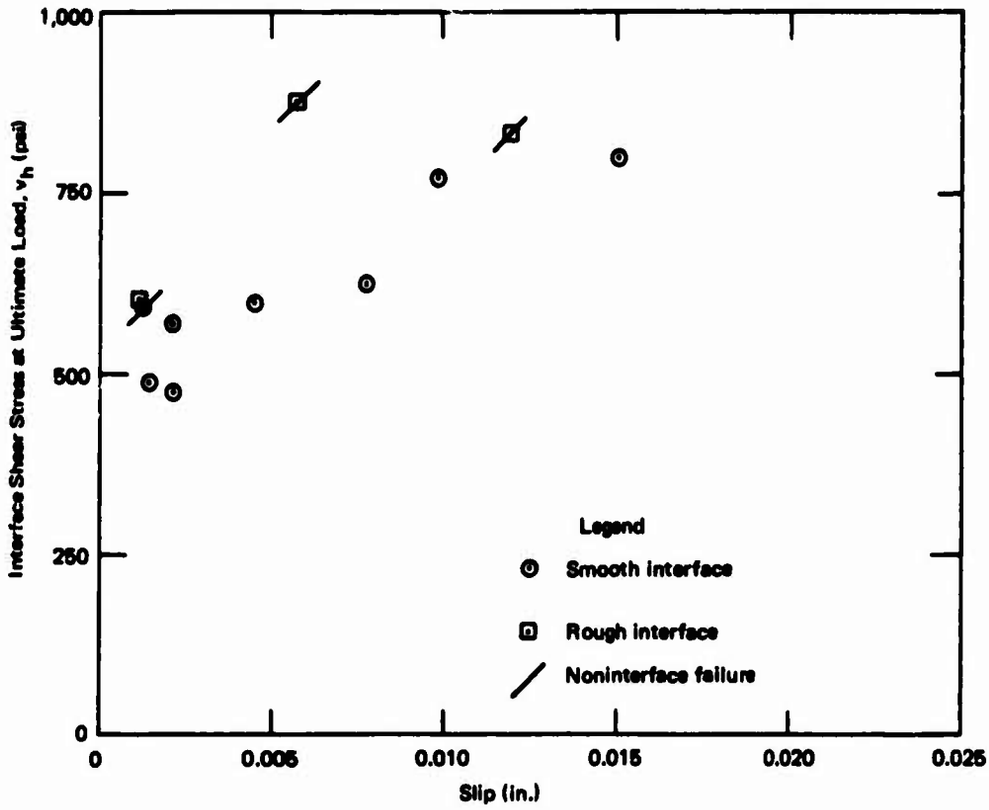


Figure 24. Interface shear stress versus slip at maximum load.

For beams with $r < 0.41\%$, after maximum load was attained, the resistance dropped to less than half of the maximum load. Increasing the stirrup ratio resulted in higher resistance after maximum load was attained even though slip became excessive. For example, beam S0.92B1 supported 80% of the maximum load while enduring slip in excess of 0.18 inch. Slips greater than 3/16 inch were observed after maximum load before spalling of concrete or rupturing of stirrups.

## SUMMARY AND CONCLUSIONS

Although the specimens were limited in number, the following observations were noted:

1. Three major types of failures were encountered: interface shear, diagonal tension, and flexure.

2. Prior to the initiation of slip, beam behavior did not depend on the amount of web reinforcement crossing the interface or the interface roughness. Initial and maximum recorded slip were found to occur between the middle of the shear span and the neighboring load point. Before initial flexural cracking, recorded slip was very small and usually did not exceed 0.0001 inch.

3. Interface cracking developed as an extension of diagonal tension cracking in the cast-in-situ elements.

4. Interface slip initiated after the interface shear stress exceeded 300 psi. Interface roughness and percent of web reinforcement had little, if any, effect on the value of shear stress at the initiation of slip. The effects of r and interface roughness became significant only after initiation of slip. The rate of slip decreases with interface roughness and with increasing r. After slip reached a value which varied from 0.0005 to 0.0011 inch, the rate of slip increased and beams with few or no stirrups crossing the interface failed almost immediately.

5. Roughness of the interface surface accounts for approximately 100 psi more shear strength above that of smooth interfaces. The shear strength of the concrete-to-concrete interface with a/d equal to 2.66 appeared to be 480 psi for smooth interfaces and 590 psi for roughened interfaces.

6. Despite appreciable slip at the interface, the full ultimate moment-carrying capacity was developed in the beams with rough interfaces and r greater than 0.61%. For smooth interfaces, the beam with r equal to 1.04% reached the predicted ultimate flexural load but failed because of interface shear. The full flexural resistance could be developed even when slip within the shear span was as high as 0.015 inch. The slip at which failure occurred increased with interface roughness and as r increased.

7. For equal values of r, the size of web steel did not influence the interface shear resistance. This was observed when the stirrup spacing was as high as 4.5 times the web width.

8. The ultimate interface shear resistances determined from the tests were higher than those recommended by the ACI code.

## DESIGN RECOMMENDATIONS

It is recommended that the relative slip between the cast-in-situ and precast elements be kept to a minimum by roughening the interface surface. The interface slip should not exceed 0.001 inch. Although the design allowables of Chapter 17 of the ACI building code[9] appear to be quite conservative,

they are recommended for safe prediction of the ultimate interface shear strength because of the lack of knowledge of the effect of the ratio of shear span to depth. The test results indicate that the ACI allowables will reduce the possibility of interface cracking and will keep the relative slip between cast-in-situ and precast elements less than 0.001 inch.

## REFERENCES


1. Naval Civil Engineering Laboratory. Technical Report R-707: Ultimate horizontal shear strength of prestressed split beams, by S. B. Nosseir and R. N. Murtha. Port Hueneme, Calif., Jan. 1971.

2. A. Amirikian. "Split-beam prestressing," Navy Civil Engineer, vol. 4, no. 11, Nov. 1963, pp. 35-39.

3. Naval Civil Engineering Laboratory. Technical Report R-564: Mix design for small-scale models of concrete structures, by D. S. Fuss. Port Hueneme, Calif., Feb. 1968. (AD 664956)

4. J. C. Saemann and G. W. Washa. "Horizontal shear connections between precast beams and cast-in-place slabs," American Concrete Institute, Journal, Proceedings, vol. 61, no. 11, Nov. 1964, pp. 1383-1409.

5. N. W. Hanson. "Precast-prestressed concrete bridges, pt. 2. Horizontal shear connections," Portland Cement Association, Research and Development Laboratories, Journal, vol. 2, no. 2, May 1960, pp. 38-58. (PCA Development Bulletin D35)

6. A. H. Mattock and P. H. Kaar. "Precast-prestressed concrete bridges, pt. 4. Shear tests of continuous girders," Portland Cement Association, Research and Development Laboratories, Journal, vol. 3, no. 1, Jan. 1961, pp. 19-46. (PCA Development Bulletin D45)

7. P. W. Birkeland and H. W. Birkeland. "Connections in precast concrete construction," American Concrete Institute, Journal, Proceedings, vol. 63, no. 3, Mar. 1966, pp. 345-368.

8. R. F. Mast. "Auxiliary reinforcement in concrete construction," American Society of Civil Engineers, Proceedings, Journal of the Structural Division, vol. 94, no. ST6, June 1968, pp. 1485-1504.

9. American Concrete Institute. Committee 318. "Proposed revision of ACI 318-63: Building code requirements for reinforced concrete," American Concrete Institute, Journal, Proceedings, vol. 67, no. 2, Feb. 1970, pp. 77-184.

10. R. H. Evans and H. W. Chung. "Horizontal shear failure of prestressed composite T-beams with cast-in-situ lightweight concrete deck," Concrete, vol. 3, no. 4, Apr. 1969, pp. 124-126.

## LIST OF SYMBOLS

| | |
|---|---|
| $A$ | Transferred cross-sectional area of composite section (in.$^2$) |
| $A_s$ | Area of prestressing steel (in.$^2$) |
| $A_v$ | Total area of web reinforcement across interface (in.$^2$) |
| $A_v'$ | Total area of web reinforcement (in.$^2$) |
| $a$ | Length of shear span (in.) |
| $b$ | Width of compression face (in.) |
| $b'$ | Width of web (in.) |
| $D$ | Diameter (in.) |
| $d$ | Effective depth of composite cross section measured from extreme compressive fiber to centroid of prestressing steel (in.) |
| $d_c$ | Effective depth measured at midspan (in.) |
| $d_s$ | Effective depth measured at midshear span (in.) |
| $E_{ct}$ | Concrete modulus of elasticity of cast-in-situ element at time of testing which was calculated from $58{,}000\sqrt{f'_c}$ (psi) |
| $E_{pt}$ | Concrete modulus of elasticity of precast element at time of testing (psi) |
| $F_{se}$ | Force in prestressing strand measured at time of testing (kips) |
| $F_{si}$ | Force in prestressing strand at time of casting the cast-in-situ element (kips) |
| $F_{sj}$ | Force in prestressing strand at time of completion of prestressing operations (kips) |
| $f'_c$ | Concrete compressive strength as determined from standard 6 x 12-inch cylinder tests (psi) |
| $f_{se}$ | Stress in prestressing strand produced by $F_{se}$ (ksi) |
| $f_{si}$ | Stress in prestressing strand produced by $F_{si}$ (ksi) |
| $f_{sj}$ | Stress in prestressing strand produced by $F_{sj}$ (ksi) |
| $f_t$ | Concrete splitting tensile strength as determined from tests of 6 x 12-inch cylinders (psi) |
| $f_y$ | Yield strength of reinforcing steel (ksi) |
| $I$ | Moment of inertia of transformed composite section (in.$^4$) |
| $P$ | Total of the two equal externally applied loads (kips) |
| $P_c$ | Measured load at initiation of flexural cracking (kips) |
| $P_u$ | Maximum applied load resisted by test beams (kips) |
| $P_{uf}$ | Theoretical ultimate flexural load (kips) |
| $p$ | Percentage of prestressing steel $\left(= \frac{A_s}{bd_c} \times 100\right)$ |
| $Q_i$ | Moment of transformed area about interface between beam element (in.$^3$) |
| $Q_m$ | Moment of transformed area about centroidal axis of composite section (in.$^3$) |
| $r$ | Percentage of web reinforcement across interface ($= 100A_v/b's$) |
| $r_l$ | Percentage of web reinforcement ($= 100A_v'/b's$) |
| $r_g$ | Radius of gyration of composite transformed section (in.) |
| $s$ | Spacing of stirrups (in.) |
| $t_c$ | Total depth of composite section at midspan (in.) |
| $t_s$ | Total depth of composite section at midshear span (in.) |
| $V$ | Shear force (kips) |
| $v_h$ | Interface shear stress, $VQ/Ib'$ (psi) |
| $v$ | Average shear stress, $V/b'd$ (psi) |
| $w_c$ | Deflection of initial flexural cracking (in.) |
| $w_u$ | Deflection at maximum load (in.) |
| $\phi$ | Angle of internal friction (deg) |

Unclassified
Security Classification

**DOCUMENT CONTROL DATA - R & D**

*(Security classification of title, body of abstract and indexing annotation must be entered when the overall report is classified)*

| | |
|---|---|
| 1. ORIGINATING ACTIVITY (Corporate author)<br>Naval Civil Engineering Laboratory<br>Port Hueneme, California 93043 | 2a. REPORT SECURITY CLASSIFICATION<br>Unclassified<br>2b. GROUP |

3. REPORT TITLE

INTERFACE SLIP BEHAVIOR OF COMPOSITE PRESTRESSED CONCRETE BEAMS

4. DESCRIPTIVE NOTES (Type of report and inclusive dates)

Not final; September 1969—July 1970

5. AUTHOR(S) (First name, middle initial, last name)

S. B. Nosseir and G. E. Warren

| | | |
|---|---|---|
| 6. REPORT DATE<br>April 1971 | 7a. TOTAL NO. OF PAGES<br>41 | 7b. NO. OF REFS<br>10 |
| 8a. CONTRACT OR GRANT NO.<br>b. PROJECT NO. YF 38.534.001.01.009<br>c.<br>d. | 9a. ORIGINATOR'S REPORT NUMBER(S)<br>TR-721<br>9b. OTHER REPORT NO(S) (Any other numbers that may be assigned this report) | |

10. DISTRIBUTION STATEMENT

Approved for public release; distribution unlimited.

| | |
|---|---|
| 11. SUPPLEMENTARY NOTES | 12. SPONSORING MILITARY ACTIVITY<br>Naval Facilities Engineering Command<br>Washington, D. C. 20390 |

13. ABSTRACT

This report deals with the interface shear strength and slip behavior of posttensioned concrete composite beams. The interface between the two composite elements was positioned on the centroidal axis of the composite cross section. Eleven simply supported beams with 8-foot spans were statically loaded to failure. The effect of interface roughness and web reinforcement on relative slip between the composite elements was studied. Web reinforcement crossing the interface and roughness of interface decreased the rate of relative slip and allowed increased magnitudes of slip before failure. Interface roughness and web steel improved the integrity, strength, and energy-absorption capacity of the composite beams. The ultimate interface shear resistances determined from the tests were higher than those recommended by the ACI code.

DD FORM 1 NOV 65 1473 (PAGE 1)

S/N 0101-807-6801

Unclassified
Security Classification

Unclassified
Security Classification

| 14 KEY WORDS | LINK A ROLE | LINK A WT | LINK B ROLE | LINK B WT | LINK C ROLE | LINK C WT |
|---|---|---|---|---|---|---|
| Shear transfer (concrete to concrete) | | | | | | |
| Concrete beams—composite | | | | | | |
| Split-beam prestressing | | | | | | |
| Slippage | | | | | | |
| Horizontal shear strength | | | | | | |

DD FORM 1 NOV 65 1473 (BACK)
(PAGE 2)

Unclassified
Security Classification